Metallic Filters for Hot Gas Cleaning

Report No.
COAL R239
DTI/Pub
URN 04/699

March 2004

by

P Kilgallon, N J Simms, J E Oakey and I Boxall

Power Generation Technology Centre
Cranfield University,
Cranfield,
Bedfordshire
MK43 0AL

Tel: 01234 754258
Email:
John.oakey@cranfield.ac.uk

The work described in this report was carried out under contract as part of the DTI Cleaner Coal Research and Development Programme. The programme is managed by Mott MacDonald Ltd. The views and judgements expressed in this report are those of the contractor and do not necessarily reflect those of the DTI or Mott MacDonald Ltd

First published 2004

Cranfield UNIVERSITY

Power Generation Technology Centre

METALLIC FILTERS FOR HOT GAS CLEANING

Final Report for DTI Cleaner Coal Programme

Project 201

Report No. PGTC/0044

March 2003

Power Generation Technology Centre

Cranfield University, Cranfield, Bedfordshire, MK43 0AL

&

Microfiltrex – a Division of the Porvair Filtration Group Ltd.

Fareham Industrial Park, Fareham, Hampshire, PO16 8XG

METALLIC FILTERS FOR HOT GAS CLEANING

P Kilgallon, N J Simms and J E Oakey, Power Generation Technology Centre,
Cranfield University, UK
Ian Boxall, Microfiltrex, UK

SUMMARY

Hot gas filtration has not only been adopted as an essential system component in hybrid technologies like the Air Blown Gasification Cycle, but is also being used to remove particulate prior to water scrubbing of fuel gases in first generation Integrated Gasification Combined Cycle (IGCC) plants. The unreliability of the ceramic filter elements in demonstration trials and the high capital cost of these particle removal systems have hindered their application and are factors restricting the uptake of gasification power plants in general. The successful development of a durable metallic filter system for the Air Blown Gasification Cycle (ABGC) would be a major step towards its implementation. Metallic filter elements have potential applications in all IGCC systems and in other industries requiring hot gas cleaning.

This project aimed to identify the optimum materials for the various component parts of metallic filter elements, evaluate candidate fabrication routes and determine likely service lives in gasifier hot gas path environments typical of IGCC and ABGC.

A screening test (Activity A) was carried out to aid the selection of candidate materials for exposure in the main materials test programme (Activity B). The materials chosen for inclusion in the second phase tests were: Haynes D205 EN2691, Fecralloy, Haynes HR160, IN690, Haynes 188, AISI 310, IN C276, Hastelloy X, IN Alloy 800HT, AISI 316L and Iron Aluminide. Activity B tests were carried out in two environments, simulating high sulphur content IGCC fuel gas and low sulphur content ABGC fuel gas. The materials were evaluated at temperatures of 450, 500 and 550ºC for the high sulphur gas and at 550ºC for the low sulphur gas, for periods up to 3000 hours.

Using the results of Activity B, existing corrosion life prediction models for gasification environments developed at Cranfield University, have been modified and used to predict the expected service lives under operational IGCC/ABGC filter conditions (Activity C). The design requirements for a prototype element for IGCC/ABGC applications have been identified and related to the data produced in this project (Activity D).

When compared to the ABGC gas environment, the IGCC gas environment has been shown to cause significantly greater damage. The damaging effect of deposit coatings has also been demonstrated. The materials tested in Activity B have been ranked in order of degree of oxidation and Haynes D205 EN 2691, Fecralloy and HR 160 have shown the best performance.

The project has provided the basis for new opportunities for the development of metallic filter media in gasification environments. To confirm this potential the manufacture of full sized elements is required together with their demonstration in pilot scale trials and in commercial installations. In addition to coal, biomass gasification can benefit from the improved reliability and filtration performance offered by metallic filters and it is recommended that further work is undertaken to evaluate materials suitable for operating in such environments.

CONTENTS

METALLIC FILTERS FOR HOT GAS CLEANING

1. INTRODUCTION

Diverse ranges of advanced power generation systems, based on the gasification of coal and associated fuels, are being developed around the world [1-5]. Hot gas cleaning technologies for gasification systems offer the potential of a lower cost approach to pollutant control, leading to simpler cycle configurations with associated efficiency advantages. Hot gas filtration has not only been adopted as an essential system component in hybrid technologies like the Air Blown Gasification Cycle (ABGC), but is also being used to remove particulate prior to water scrubbing of fuel gases in first generation Integrated Gasification Combined Cycle (IGCC) plants. The unreliability of the ceramic filter elements in demonstration trials and the high capital cost of these systems have hindered their application and are factors restricting the uptake of gasification power plants in general. The successful development of a durable metallic filter system for the ABGC would be a major step towards its implementation. Metallic filter elements have potential applications in all IGCC systems and in other industries requiring hot gas cleaning.

2. OVERALL AIM

This programme is aimed at identifying the optimum materials for the various component parts of metallic filter elements, evaluating various fabrication methods and determining their likely service lives in typical gasifier systems.

Specific objectives are to:

- assess the performance of new metallic fibre, sintered metal powder and wire materials suitable for the manufacture of metallic filter elements and investigate the effects of fabrication methods on service performance.
- determine the maximum operation temperatures and fuel gas contaminant levels for an optimised metallic filter system.
- extend existing life prediction models to encompass the filter materials and make preliminary predictions of service lives in IGCC, ABGC and related applications, e.g. biomass gasification.
- design a prototype element for IGCC/ABGC applications.

3. BACKGROUND

Around the world a diverse range of advanced power generation systems are being developed that are based on the gasification of coal and associated fuels [1-5]. IGCC systems have reached the demonstration stage in Europe, with plants in Holland (at Buggenum [6]) and Spain (at Puertollano [7]) both based on oxygen blown entrained flow gasification processes. In the UK, the ABGC system continues to be investigated although an ABGC system demonstration plant has yet to be built. Elsewhere, the USA in particular has an extensive programme for the demonstration of gasification technologies.

The development and introduction of hot gas cleaning (HGC) technologies offer the potential of a lower cost approach to pollutant control, leading to simpler cycle configurations with associated efficiency advantages. Hot gas filtration has not only been adopted as an essential system component in hybrid technologies like the ABGC, but is also being used to remove particulates prior to water scrubbing of fuel gases in first generation IGCC plants. The filters currently employed are based on the designs developed for pressurised fluidised bed combustion applications in the 1980s using

ceramic filter elements. The unreliability of the ceramic filter elements in demonstration trials and the high capital cost of these systems have hindered their application and are factors restricting the uptake of gasification power plants in general.

The hot gas filtration systems need to operate in aggressive gasification environments at 250-700°C and at pressures of 10-25 bar_g, depending on the particular gasification system. In order to realise fully the cost and environmental advantages, it is essential that the systems provide not only efficient contaminant removal but also have the reliability and availability required of the overall system. Over the years, adaptations to system configurations and more realistic expectations of filter performance have led to the original choice of ceramics for the filter medium being questioned. It is now apparent that reliable, lower cost filter systems can be operated using metallic filter media, provided improved materials selection and advanced fabrication methods are developed. Metallic filter media provide a number of significant advantages over ceramics:

- Lower pressure drop leading to a reduced filtration area and hence reduced capital cost
- Excellent cleanability
- More predictable durability and reliability
- Simpler installation and handling requirements

The potential for fuel gases to cause sulphidation, erosion and fouling raises concerns over the selection of materials and the lifetimes of filter components, similar to those for the heat exchanger which is used to cool the fuel gas before the hot gas cleaning stages. Also down-time corrosion, resulting from deposits of particles and condensates which develop during operation, may lead to severe pitting damage and stress corrosion cracking.

Microfiltrex is a world class manufacturer of metallic filter media for a wide range of applications. In recent years, trials have been carried in conjunction with a major US IGCC demonstration project to evaluate the potential of metallic filter elements in these systems using filter elements made from traditional materials used previously for other applications. These trials, which have lasted for several thousands of hours, have confirmed the benefits indicated above. However, they have also highlighted the problems of using metallic media in such aggressive environments due to the highly corrosive nature of the fuel gas and the deposition of condensates within the filter element's structure. As the success of metallic filter media is dependent on achieving an economic life while ensuring adequate filtration performance and reliability, optimisation of materials selection and fabrication methods for IGCC/ABGC applications is required

4. EXPERIMENTAL

4.1. Activity A – Materials Selection And Screening

4.1.1. Introduction

The range of fibrous and wire materials currently used in filter applications were reviewed and the best candidates selected for a corrosion screening test in a typical IGCC high sulphur coal fuel gas environment at 450°C for 1000 hours. The selection process for the candidate materials for the initial screening test was based on:

- Data available from the performance of existing metallic filter elements and other hot gas path components in various gasification systems; this included a site visit to a major USA facility by Microfiltrex staff.
- Published and in-house alloy performance data in gasification environments.
- Recommendations from suppliers of high performance alloys such as Haynes, Special Metals and Resistalloy.

- The commercial viability of scale-up and technical feasibility of fabricating the alloys into filter element parts.

These materials covered Iron, Nickel and Cobalt based alloys and included a number of welded specimens. Baseline alloys were also included to provide an indication of the relative corrosive nature of the environment. The list of materials included in the screening test is given in Table 1 along with a nominal chemical composition. Materials were tested in forms relevant for filter manufacture such as with a weld or pre-treatment such as pre-oxidation. The environments used in the corrosion testing have been determined from work under a parallel project supported by the DTI (Project Number 110).

Before exposure each specimen was measured, washed/degreased and weighed. The dimensions of the cap and root of welds on welded specimens were not measured and therefore are not included in the calculation of surface area.

4.1.2. Experimental

The conditions for the screening test provided a relatively severe but realistic simulated gasifier gas for a hot gas filter in an IGCC system. Specimens were exposed for 1000 hours at 450°C (Table 2) to a gas simulating that produced by an oxygen blown entrained flow gasifier with no sulphur removal prior to the filter (this high H_2S gas composition is given in Table 3). The furnace arrangement used is shown in Figure 1. At the start of the test the furnace was flushed with nitrogen to remove the air before the test gas was added. The components of the test gas were supplied from two gas cylinders and mixed at the top of the furnace. The moisture was added to the gas mixture by bubbling the gas from the hydrogen sulphide/carbon monoxide cylinder through deionised water at laboratory temperature. Prior to the furnace cooling at the end of the test it was again flushed with nitrogen to remove the test gas and avoid acid dewpoint corrosion.

4.1.3. Weight Change Results

The specimen holder was unloaded from the furnace, allowed to cool in air and the specimens removed and placed into a dessicator before weighing. Each specimen was visually inspected to assess the amount of corrosion product lost during exposure, unloading and weighing. For a number of specimens it was clear that significant amounts of the corrosion product layer had spalled, as demonstrated by the AISI 316L specimen in Figure 2. The weight change per unit area data is ranked in Table 4 and includes comments on the reliability of each measurement in relation to corrosion product remaining.

4.1.4. Corrosion Measurements

Before the specimens were sectioned they were encased in a thin layer of resin (Struers Epofix) to protect the corrosion product layers during cutting. The sections were then cold mounted in resin before grinding and polishing to a 1μm finish. Each section was then viewed using an optical microscope to measure the thickness of the oxide and sulphide layers and identify any other features related to the exposure (e.g. Figure 3). The results of measurements made together with comments are given in Table 5.

4.2. Activity B – Performance Assessment

4.2.1. Introduction

Results from the screening test (described above) were used to aid the selection of candidate materials for Activity B. The materials from the screening test recommended for inclusion in the remaining tests were: Haynes D205 EN2691, Fecralloy, HR160, IN690, HA188, INC276, Hastelloy X and AISI316L (as well as IN800HT and AISI310 reference materials). A number of 'new' materials under development were also identified and where suitable product forms were available they were included in the later tests. Therefore, iron aluminide is among the list of selected materials given in Table 6. For this part of the project, attention was paid to testing the materials in the correct product forms, with treatments used in element manufacture as these may promote a different balance of damage

mechanisms that could initiate premature failure. Fabricated parts were also included in this task so that the effects of the methods used to manufacture elements could be assessed.

Two environments, simulating high sulphur content IGCC fuel gases (generated from high sulphur coals and petroleum coke) and low sulphur content fuel gases (such as cleaned coal-derived fuel gas, ABGC fuel gas, biomass or co-fired coal and biomass fuel gases), were used in this part of the test programme. The materials were evaluated at temperatures of 450, 500 and 550ºC for the high sulphur gas and at 550ºC for the low sulphur gas, for periods up to 3000 hours. Deposits were added with a re-coat interval of 1000 hours to simulate the effects of the deposits that are known to occur in such filter systems.

4.2.2. Experimental

Four tests were carried out as part of Activity B as shown in the test matrix given in Table 2. Each of the four tests started with 13 specimens as detailed in Table 6. Specimens were exposed for up to 3000 hours at 450-550°C (Table 2) to either the high H_2S (= IGCC) or low H_2S (= ABGC) concentration simulated gases (compositions are given in Table 3).

The general experimental procedure was the same as that used for Activity A but with simulated deposits being applied to samples. These deposits were produced by mixing the dry deposit components together with propan-2-ol to produce a slurry. This slurry was applied to one side of the weighed test specimens and reweighed after the solvent had evaporated before testing. For wire specimens approximately one half of the wire was coated. For the mesh and fibre specimens deposit coated and uncoated specimens were used. The recoat interval was 1000 hours which meant that in tests 2, 3 and 4 (all 1000 hour duration) the deposit were applied only at the start of the test, whereas test 1 (3000 hour duration) had deposit applied at 0, 1000 and 2000 hours.

Tests 1, 2 and 4 (high H_2S gas and applied deposit) were carried out in two linked gastight horizontal furnaces as shown in Figure 4. At the start of the test or after deposit recoating the samples were placed into the cold furnace. The furnace was flushed with nitrogen during heat-up to remove air and when it had reached the test temperature the test gas flow was started. The components of the test gas were supplied from two gas cylinders (HCl/H_2 and $CO/CO_2/H_2S$) and mixed at the top of the furnace. The moisture was added to the gas mixture by bubbling the gas from the hydrogen sulphide/carbon monoxide/carbon dioxide cylinder through deionised water at laboratory temperature. Prior to furnace cooling, for either deposit recoating or sample removal at the end of the test time, flushing with nitrogen was used to remove the test gas and avoid acid dewpoint corrosion during cooling.

Test 3 (low H_2S gas and applied deposit) was carried in a vertical gastight furnace arrangement shown in Figure 1. The test procedure is as above except that the two gas cylinders were $HCl/H_2/N_2$ and $CO/CO_2/H_2S/CH_4/N_2$ and the moisture was added to this gas mixture by bubbling the gas from the hydrogen sulphide containing cylinder through deionised water at a temperature of 47°C (as the target ABGC gas is wetter than the target IGCC gas).

The weight change data for Activity B could not be used as the primary measure of corrosion damage as the following factors demonstrate.

1. Samples were not in crucibles during testing so spalled corrosion product and/or deposit was not measurable.
2. Surface areas for a number of specimen types would be difficult to measure/calculate e.g. sintered metal powder (SMP) specimens.
3. Many samples were only deposit coated on one side so the weight change would include both coated and uncoated areas.

For samples where the substrate was tested deposit coated and uncoated some comparisons can be made using weight change data. However, for most samples optical measurements of oxide thickness

on cross sections were used (sulphide layer thickness not used) to assess metal damage and allow comparisons to be made.

4.2.3. Corrosion Measurements

The primary measure of corrosion damage was optical measurements of metallographic cross sections. The exposed samples from each test were cold mounted in resin (Struers Epofix) to maintain the integrity of the corrosion layers during cutting of cross sections. The sections were then cold mounted, ground and polished. Typical and observed maximum oxide thicknesses were measured for each sample using an optical microscope with a measurement resolution limit of approximately 1µm. Measurements were made on both the areas exposed to the gases through the applied deposits and also areas that were not deposit coated.

The oxide thickness data for Tests 1-4 are given in Table 8 (with applied deposit) and Table 9 (without applied deposit). This data is also shown graphically for each test as bar charts in Figures 5-12 with the materials placed in the order of their performance ranking (In Test 1 Hastelloy X sample was removed after only 2000 hours and this is reflected in the ranking). The materials were ranked by typical oxide thickness (and maximum values for materials with equal typical measurements), these rankings are given in Tables 10 and 11. It is worth noting that for some material forms e.g. SMP's that the maximum oxide thickness measurable would be limited by the particle size. Where a whole particle had oxidised the oxide thickness was taken as half the particles width. Figures 13-15 show cross sections where this has occurred. Figure 15 shows a cross section for Iron Aluminide and whilst the maximum oxidation is effectively half the particle size it is clear that large regions of the material have been attacked

In addition Tables 10 and 11 compare the ranking made for materials in Activity A (IGCC - High H_2S gas) that were used in the Activity B tests and also have a mean ranking for Tests 1, 2 and 4 (IGCC - High H_2S gas) in Activity B. In general the ranking of materials tested in the high H_2S gas correspond with those given in Activity A with the exception of IN690 which was highly ranked in the screening test but has shown poor performance in latter tests.

The damage in Test 3 (ABGC - low H_2S gas) is significantly less than the equivalent IGCC high H_2S gas test (Test 2). The ranking of materials for test 3 is not as defined as for the other tests as the damage was slight and for many materials was below the measurement limit of the optical microscope.

In general, for all test conditions the damage was greatest on the deposit coated side of the specimens as demonstrated by Figures 5-12.

4.3. Activity C - Modelling and Determination of Operating Constraints

4.3.1. Introduction

The development of models to allow prediction of materials performance in gasification systems, for many of the complex synergistic modes, is limited by the data available. However, for isothermal corrosion in gaseous gasification conditions, a large amount of materials performance data has now been generated from a number of laboratories and this is enough to model the performance of at least some materials in such conditions.

A framework isothermal corrosion model for gasifier hot gas path conditions was developed previously for an EC JOULE programme and applied to Alloy 800H and AISI 310 [8]. The models were based on materials performance data available during the programme and published literature data. Sets of approximately 30 data points were obtained from BCC, JRC Petten, KEMA, ENEL and EPRI covering the temperature ranges 500-900°C (though at some temperatures only single data points were available). The models were based on an assumption that gaseous corrosion in gasifier product gases followed parabolic kinetics and was either oxidation or sulphidation:

$$\log Kp = A + B \times R + C/T$$

where, R is the oxygen excess parameter [9, 10],

$$R = 1.5 \log\, pO_2 - \log\, pS_2 + D/T + E$$

where *A, B, C, D* and *E* are alloy specific constants; *T* is the metal temperature in Kelvin.

Another model for gaseous gasifier product gas corrosion is reported in the literature. This model has been produced by Shell during development of their oxygen blown 'full' gasification system [11, 12] and is targeted only at the gas compositions anticipated for that process. The mathematical form of this model is not fully available, but it is known that for high alloy steels parabolic rates constants are calculated (for exposures in excess of 500 hours) using pS_2, pO_2 and temperature, and that

$$Kp \propto \left(pS_2 / pO_2^{3/2} \right)^x$$

For modelling isothermal gaseous corrosion for this project, a much larger set of materials performance data is now available. Unfortunately, most of the data is available only in the form of mass change data. This means that more extensive data sets, of up to 100 points for the more commonly researched alloys, are available for producing models of average corrosion damage. More limited data sets, up to ~40 points, are available for producing maximum damage models.

After analysing the data sets now available, it was found that the best model for the dependence of corrosion rate on gas composition and temperature took a logistic, or sigmoidal, form (e.g. Figure 16 shows the form for AISI 310):

$$Corrosion\,Rate = \frac{a - d}{1 + \left(\dfrac{\log\, pS_2 - 1.5 \log\, pO_2}{c} \right)^b} + d$$

where, *a*, *b*, *c* and *d* are temperature dependent constants of the form,

$$a = a_o \exp\left(-Q_o / T\right)$$

where *T* is the metal temperature in Kelvin; a_o and Q_a are constants. In theory, the constants *a* and *d* should also be slightly dependent on the pO_2 and pS_2 levels, but the corrosion data currently available is not sufficiently detailed to show this effect.

This form of the model compares well with the lower end of the data generated by Shell for their gasification process, where the corrosion rate increases rapidly in the oxidation/sulphidation regime with increasingly sulphidising conditions and then increases more slowly on entering the sulphidising regime. It should be noted that the ABGC process operates under somewhat more oxidising conditions around the change from the oxidation regime to the rapidly increasing oxidation/sulphidation regime.

4.3.2. Results

Using the results of Activity B, the existing corrosion life prediction models developed at Cranfield have been modified and used to predict the expected service lives under operational IGCC filter conditions. This has allowed the upper temperature limits to be established for the various materials under operational conditions specified for each plant type/fuel combination.

The maximum oxide measurements have been used in the model to produce the graphs shown in Figures 17 (with deposit) and 18 (without deposit). Typical oxide measurements have been used to produce the plots in Figures 19 (with deposit) and 20 (without deposit). These plots allow preliminary predictions of service lives in IGCC, ABGC and related applications for the materials studied in this

project. The plots can aid filter media material selection if an upper corrosion rate limit is set for a known gasifier environment and operating temperature. The corrosion rate allowances are determined by economic factors (e.g. cost of replacement filter elements, viability of power generation process, etc.), but an initial minimum requirement for large scale coal fired power generation is that the filter elements last for at least one year. The upper corrosion rate limit will therefore initially be formulated from the required operational life of the filter (one year) and the failure criteria for the filter media type.

The latest filter element designs incorporate several different metallic parts each with different requirements in terms of strength and corrosion resistance resulting in each part having a different failure criterion. For example, the diameter of fibres in a SMF filter are typically 1.5-40 µm and could have a failure criteria of 50% loss, whereas the support structure can be several millimetres thick and a failure criteria of 1mm.

Corrosion rate data can also be used to estimate life of the filter where the life is limited by a reduction in the porosity of the filter media by oxide scale growth. This life criteria is more applicable to filters manufactured from SMP than fibres. An example plot for SMP media showing the effect of two corrosion rates on the pressure drop across the filter with time is shown in Figure 21 (the parameters used for the calculation are given in Table 12). Life prediction models for SMF and SMP filter media are discussed further in section 4.4.4.4.

Using the corrosion allowance failure criteria above and an operational life of one year (8760 hours) the upper corrosion rate limit would be of 0.00223 µm/hour for a 40 µm diameter fibre and 0.114 µm/hour for a support structure. The corrosion rate limit for the fibre is shown as a dotted line on Figure 17 (maximum measured damage for deposit coated specimens) which also has the groups of data that correspond to each test condition indicated. This Figure indicates that Fecralloy, Haynes 160 and Haynes D205 are the only candidate materials for fibre media under IGCC conditions at 450ºC. Under ABGC conditions at 550ºC candidate materials for fibre media are Hastelloy X, Alloy 800, Fecralloy and Haynes 160. All materials tested, except for IN690 under IGCC conditions at 500 and 550ºC, are candidate materials for structural components under all test conditions.

The analysis above illustrates how the maximum working temperature for candidate materials can be identified for each test gas. However, there are economic arguments that may be put forward to reduce the upper working temperature to increase filter lives and plant reliability. Additionally, the actual failure criteria used for filter components are commercially sensitive so example values have been used in the analysis that will differ from those used by filter manufacturers.

4.4. Activity D - Filter Element Design

By far the most common barrier filtration configuration used in hot gas cleaning for power generation is the filter candle, where dirty gas flows from the outside to the inside of the candle wall, and contaminant which accumulates on the surface is regularly removed by pulsed-jet cleaning. Such filter systems are widely viewed as the best prospects for hot-gas cleaning in clean-coal power plants, from both a technical and economic point of view (see later), and Microfiltrex have based their development work around improving the performance of such filter candles.

4.4.1. Filtration Requirements

It is commercially vital that a power plant operates at a high availability, since a four or five day shutdown for e.g. a broken element could cost as much as £2m, so the requirements in the following list relating to element integrity are essential.

4.4.1.1. High Temperature Stability

The filter medium must be able to survive for many thousands of hours at high temperature (in the range 350-550 ºC for gasification systems) without degradation or embrittlement.

4.4.1.2. Thermal & Mechanical Shock Resistance
Thermal transients occur in the filter system on PFBC and gasification plants, sometimes due to backpulsing with gas at a lower temperature (though some gasification systems can re-cycle fuel gases for back pulsing), and sometimes due to incompletely burned coal transferring to the surface of a filter candle and igniting there, and a filter candle must be able to survive such events.

Mechanical damage to a filter element can occur during transportation, installation in the tubeplate and during a maintenance shutdown (perhaps to replace another element, which is already damaged) so adequate strength and fracture toughness is required.

4.4.1.3. Vibration Resistance
Large-scale industrial plant where heavy machinery is operating is subject to many sources of vibration and filter elements must be able to survive in this environment for thousands of hours.

4.4.1.4. Corrosion Resistance
Prolonged exposure at elevated temperatures carries with it the risk of oxidation, leading to embrittlement and the risk of element failure. The hot-gases in coal fired power plants are potentially corrosive, especially due to the presence of sulphur compounds which under moist conditions (e.g. at a shutdown) can become acidic and attack any component of the filter system, so care must be taken when selecting materials of construction, especially metallic ones.

4.4.1.5. Creep Resistance
There are several configurations for filter systems and creep needs to be considered in the design of elements. For example, in a pulsed-jet candle filter system where the flanged end of the candle is fixed to the underside of a tubeplate the candle is hanging down under its own weight; this means that elongation of the element at the elevated temperatures is a possibility.

4.4.1.6. Adequate Flange Strength
Filter candles are closed at one end and at the open-end need to be fitted with a suitable flange for sealing into the tubeplate without the risk of leaks. Since this is the mechanical fixing point, and lateral mechanical forces on the candle can occur, it must be designed with maximum strength.
4.4.1.7. Abrasion Resistance
Since the gas contains particulate matter, travelling at high velocity, then abrasion of the surfaces in the filter, including the candle, is a risk that must be assessed and minimised. Good filter unit design avoids this.

4.4.1.8. Filtration Efficiency
Protection of the environment from particulate emissions, and the demands for high quality (clean) feed gas to downstream equipment to enable high efficiency and long life necessitate high filtration efficiency filtration with downstream emissions <1ppm.

4.4.1.9. In Situ Cleaning & Off Line Cleanability
Unscheduled Shut down of the filter, and therefore the plant, for any reason is a very expensive operation (see above) and so in situ cleaning is vital. In the case of filter candles this takes the form of a pulsed-jet cleaning system (see later).

Even a highly efficiently Pulsed Jet cleanable filter medium such as Sintered Metal Fibre will progressively become plugged over a very long time scale, such as 1 or 2 years. When this happens the candles will be removed from the vessel and chemically cleaned off line, so it is important that the candles are amenable to efficient cleaning by such means.

4.4.1.10. High Permeability
A filter medium with a high permeability is required to minimise the energy requirement to pump the gas through the filter, but this must be at a fine filtration rating to prevent particles from penetrating the medium and preventing efficient pulse-jet cleaning.

4.4.1.11. Low Downtime
As illustrated above a shutdown is expensive, so when one occurs the filter design must incorporate rapid replacement of elements, as well as ease of assembly and disassembly of the vessel.

4.4.1.12. No Ash Bridging
It is possible for ash to accumulate between filter elements instead of falling to the bottom of the vessel, and this has been reported to cause element fracture. This can be avoided by good design of the filter element layout.

4.4.1.13. Low Capital Cost/ Low Operating Cost
Clean coal generating technology has to compete with other sources of electricity and so capital cost of the plant must be competitive, and filter reliability must enable an operational life in excess of 2 years.

4.4.2. Potential filter media and the Barriers to Success

4.4.2.1. Porous Ceramics
Given the requirements for prolonged exposure to high temperatures in a potentially corrosive atmosphere, then a monolithic porous ceramic filter medium is an obvious candidate for candle filters. Hence the majority of the reported work in this area has involved such ceramic candles and they have generally been viewed as the front-runners for some time. Often the candles will have a coating of a fine layer of fibrous aluminosilicate mat, or fine SiC granules. However they are brittle and prone to crack or fracture from thermal and/or mechanical shock; they have been found to show creep; oxidation leading to further embrittlement has been found; flange fracture has occurred; permeability is low leading to high differential pressures; cleaning difficulties have been reported, and ash bridging leading to fracture has occurred.

4.4.2.2. Ceramic Fibres
A fabric filter made from ceramic fibres should have the same high temperature and corrosion performance as monolithic ceramics, but without the propensity to brittle fracture. Such fabrics can operate up to 700 - 800 ºC, but they are fragile and have lower capture efficiency than monolithic ceramics.

4.4.2.3. Continuous Fibre-Reinforced Ceramic Composites
In an attempt to add fracture toughness to monolithic ceramics, Continuous Fibre-Reinforced Ceramic Composites (CFCC's) have been prepared. However they are reported as having a reduced capture efficiency, showing oxidative embrittlement and persistent structural defects and holes, and this approach has not been pursued.

4.4.2.4. Fabric From Coated Glass Fibres
Such fabrics can be used up to ca. 480 ºC, and show a loss of strength from rough handling, high temperatures and corrosion. "Pin-holing" is a common form of failure.

4.4.2.5. Porous Sintered Metal Powders
Porous sintered metal powder (SMP) filter media has been used for many years for industrial filtration, e.g. in the polymer processing industry, where stainless steel SMP media is fabricated into leaf-disc capsules. SMP candles can operate at hot-gas temperatures and are sufficiently rugged to withstand thermal and mechanical shocks, and show no creep, but have a low permeability due to being only ca. 35% porous (i.e. have higher energy requirements) and if manufactured from AISI 316L stainless steel would suffer corrosion in a PFBC or gasification plant. As with porous granular ceramic media SMP does not perform well if used in Pulsed Jet Cleaning, and frequent shutdown is required to remove and clean the blocked candles. The low porosity structure of SMP media can be seen from the photomicrograph shown in Figure 22, particularly when compared to the structure of sintered metal fibre (Figure 23).

4.4.2.6. Sintered Metal Fibre

Like SMP a candle fabricated from sintered metal fibre (SMF) can operate at high temperatures, withstand thermal or mechanical shocks, and shows no creep, with the added advantages that it has high permeability and can be pleated, if required, to give a significant increase in area (both leading to reduced differential pressures and energy consumption, or fewer candles and a smaller filtration system). SMF is also superior to granular ceramics and SMP media in having very high pulsed jet blowback efficiency, such that a return to within 5% of the clean differential pressure can be achieved over many cleaning cycles. However, when manufactured from standard AISI 316L stainless steel such a medium shows only moderate corrosion resistance, with the high surface to volume ratio of the fine fibres decreasing their lives. An improvement in this area is required to make filter candles in SMF the ideal Particulate Control Device (PCD) for hot gas filtration in Clean Coal Technology plants.

4.4.3. Filter Candles from Sintered Metal Fibres

4.4.3.1. Media

4.4.3.1.1. Manufacture

The starting point for the manufacture of metal fibres is a wire of 0.5 mm diameter, which is drawn down, encased in a copper sheath, and then bundled together with many other such wires. The bundle of encased wires is further drawn down in multiple drawing steps until the correct fibre diameter is obtained (diameters can range from 1.5 to 40 µm). The copper sheath is leached off and the fibres are chopped into 25 mm lengths. Fibres can be manufactured in AISI 316L and AISI 304 stainless steels and a range of speciality steels. The fibres are formed into a web by either air or wet laying techniques in densities ranging from 75 to 900 g/m^2. For sintering, panels are stacked up separated by Monel mesh to prevent webs sintering to each other (sometimes 2 or 3 webs are combined together to produce a 2 or 3 layer medium), and placed in a vacuum furnace with a static load on top. The furnace is vacuumed down and heated to a temperature around 1000 ºC to form diffusion bonds between touching fibres; this produces a porous metal "paper" with the sinter bonds acting as the binder to impart strength. In order to achieve the correct filtration rating the sintered webs are pressed to a defined thickness, and tested for air permeability, thickness and weight.

4.4.3.1.2. Property advantages

Compared to a granular filter medium SMF has a high porosity (up to 85%) which means that at a given micron rating it will have a high permeability, resulting in low differential pressures; this in turn leads to low energy consumption in filtration or blowback. The sinter bonds mean that the medium is strong and resists compaction under operating differential pressures. SMF can be pleated, if required, resulting in an increased effective filtration area, which further reduces operating differential pressures, or a reduction in system size. For a pulsed-jet blowback candle it is common to use a two-layer filter medium with the coarser layer on the inside of the element to give support to the finer outer layer, which acts as a surface filter giving a much better blowback performance than either granular ceramic or SMP candles. The high porosity of SMF media can be seen in Figure 23.

As mentioned previously a filter medium from SMF makes a candle ideally suited to Hot Gas Filtration in Clean Coal Technology plants, with the exception that where the fibres are conventionally manufactured from 316L stainless steel the high aspect ratio fibres show only moderate corrosion resistance in the aggressive environment prevailing. For this reason we set out to develop a filter candle with SMF filter medium showing enhanced corrosion resistance, which would therefore represent a major step forward over the brittle candles from sintered ceramic powders which have been favoured in the past for such power generation plants. We have now developed filter candles utilising SMF media made from Nickel based and FeCrAl alloys, and as will be shown by the results given below these candles mark a significant step forward in this technology.

4.4.3.2. Candles

Filter candles, suitable for a pulsed-jet, hot gas filtration system, are constructed around a core made from a perforated tube to give support to the structure against differential pressures. The filter pack which fits around the core comprises the filter medium with a downstream mesh to support the medium over the core holes, and an upstream mesh to protect against physical damage; the pack may be pleated if a larger area is required. One end of the candle is closed and the other is open with a suitable threaded or flanged end fitting to connect to the tubeplate. The candle may be fitted with a suitable guard to give further protection against physical damage. A set of Hot Gas filter elements made using SMF media can be seen in Figure 24.

4.4.3.3. Filter system

Many of the above filter candles will be fitted into a suitable tube plate, to form a tubesheet, where the flow through all the candles is combined and flows on to the next part of the plant. The tubesheet is contained in a large pressure vessel, with the whole of this equipment comprising the filter system. In use, the surface of the filter candles will quickly become covered with a layer of dust and the differential pressure will rise and the candles will need cleaning. Because of the time/cost of removing the tubesheet from the vessel for cleaning it is advantageous to use a Clean In Place system, which in this instance means Pulsed Jet Cleaning.

As can be seen from Figure 25 the candles are fitted with a pulsed jet nozzle, whereby a short sonic pulse of gas is blown back through a predetermined number of filter elements (only some filter elements are pulsed at any one time to minimise the effect on process gas stream). The dust is dislodged and drops freely to the bottom of the vessel, from where it can be removed for disposal or recovery. The sonic pulse lasts for less than half a second ensuring that the operating process is not interrupted. High speed photography shows the action of Pulsed Jet cleaning in Figure 26.

4.4.4. Test Results

4.4.4.1. Flow Pressure Loss Characterisation

A test programme was conducted at the Microfiltrex Development Centre utilising a cold flow test rig to evaluate the performance of Metal Fibre elements for hot gas applications. SMP and SMF elements were manufactured from AISI 316L stainless steel that were suitable for cold flow atmospheric air testing. The fibre and pore structures were designed to provide equivalent performance to that utilised for high temperature service. Four Filter Elements (60mm outside diameter by 1400 mm long) were installed and initially the flow pressure loss characteristics of four different metal fibre media were determined and compared with commonly used ceramic and sintered metal powder filters providing similar filtration efficiency. The tests were conducted at ambient conditions with media superficial face velocities in the range 0.01 - 0.06 m/s, which is typical for this type of application.

The results are shown graphically in Figure 27 and clearly show the high permeability and low-pressure loss characteristics of the metal fibre media compared to ceramic and sintered metal powder materials.

4.4.4.2. Reverse Cleaning Characterisation

A SAE J726 [13] Dust feeder was connected to the test rig (Figure 28) and the filter elements were challenged with ISO 12103 fine test dust [14]. The upstream and downstream pressure transducers were connected to an HBM MP01 data acquisition system to monitor pressure build up and regeneration characteristics. The test was run for a period of approximately 2 hours until a stabilised baseline pressure loss was achieved.

Figures 29 and 30 show the pressure build up and regeneration characteristics at the initial start up and stabilised periods of the test.

The pressure loss characteristics of the filter element comprise of three basic components:

$\Delta p_{peak} = \Delta p_{clean} + \Delta p_{residual} + \Delta t_{ransient}$

Where Δp_{clean} = Clean Δp across filter element
$\Delta p_{residual}$ = Residual Δp - non-recoverable element of pressure loss attributable to depth filtration and cake binding. Additional factors include corrosion products etc.
$\Delta p_{transient}$ = Transient Δp - recoverable cake dependant on cake structure, porosity, adhesive/ cohesive properties etc.

Figure 29 shows the initial start up region where the residual pressure loss is rapidly increasing as the particulate penetrates the depth of the filter media and adheres to the surface. The metal fibre media with its fine surface structure promotes surface filtration and thus the rate of increase of the residual Δp rapidly decreases and stabilises. This is one of the most critical components in ensuring good performance in regenerable filters.

Figure 30 shows the operating performance where the filter cake is formed and Δp regenerated with each reverse clean, the baseline Δp has stabilised at approximately 1100 Pa.

The filter media structure with its high porosity enable such filters to provide substantial improvements in performance in terms of clean flow Δp and the generation of a stable baseline Δp when compared to ceramic and sintered metal powder materials. This is achieved by enabling more energy to be delivered to the cake surface.

4.4.4.3. Metallurgy

While clearly the architecture of the filter element and structure of the filter media are critical to the on-line performance of the filter element, the metallurgy of the filter media is equally as important in defining on line performance. The structural inegrity of the filter media to mainatain efficiency is clearly a must. However the build up of corrosion products, oxide scale and spalling will considerably increase the residual Δp of the filter and may ultimately blind the filter element completely. Figure 13 shows a stainless steel sintered metal powder new and post exposure to a high sulphur environment. Figure 13 clearly shows how the pores of the filter media have been blocked with corrosion product.

For many years metal filters have been extensively used in hot gas applications such as catalysts recovery where corrosion is not a significant problem and numerous products exist in materials such as AISI 316L stainless steel.

However it is corrosion resistance that has largely limited the development of metal elements for coal fired power and other advanced processes, and as a result the focus has for the past 10 - 15 years been on the development of advanced ceramics.

4.4.4.4. Life Prediction Models

Experience has shown that the life assessment of SMP and SMF filter media will be based on different methodology. SMP filter media with its relatively closed pore structure, typically 30-50%, will be life limited by oxide scale growth, corrosion spalling and blinding of the pores resulting in a reduction in the porosity of the filter medium. A life prediction model for SMP filter media is described in section 4.4.4.4.1.

SMF media has a very open pore structure (70-85%), giving high porosity, and so is arguably more tolerant of corrosion product and oxide growth in terms of its filtration and regeneration characteristics than SMP media. The small fibre diameters used for SMF media, typically 1.5 to 40 µm, are more susceptible to structural failure and total consumption than its larger powder counterpart. SMF media will be life limited by structural failure of the fibres or a steady rise in the differential pressure loss of the filter under operating conditions to an unacceptable level for plant operation. A life prediction model for SMF filter media is described in section 4.4.4.4.2.

4.4.4.4.1. Life Assessment Predictions for Sintered Metal Powder Filter Media.

Corrosion rate data can be used to estimate life of the filter where the life is limited by a reduction in the porosity of the filter media by oxide scale growth. The reduction in porosity and resulting change in pressure drop across the filter can be analysed using the Kozeny Carmen equation for laminar flow through packed porous beds. For a granular bed (or SMP filter medium)

$$\frac{\Delta P}{L} = \frac{150h.V(1-e)^2}{d^2.e^3} + \frac{1.75p.V^2(1-e)}{d.e^3}$$

$\Delta P = Pa.$ pressure loss
L = bed depth (m)
? = gas viscosity (Pas)
d = equivalent particle diameter (m)
e = voidage fraction
? = gas density (kg/m^3)

or:-

$$\frac{\Delta P}{L} = \frac{150h.V(1-e)^2}{f_s^2.d^2.e^3} + \frac{1.75r.V^2(1-e)}{f_s.d.e^3}$$

f_s is a shape factor defined by:

f_s = Surface area of a sphere with the same volume as particle
surface area of the particle

Let the factional increase in particle size be 'k' Then the solid fraction (1-e) will become, $(1+k)^3$ (1-e) and the voidage fraction 'e' will become $1-(1+k)^3(1-e)$ then, $\frac{(1-e)^2}{d^2.e^3}$ will become

$$\frac{\left[(1+k)^3(1-e)\right]^2}{d^2(1+k)^2\left[1-(1+k)^3(1-e)\right]^3} = \left[\frac{(1+k)^2(1-e)}{d}\right]^2 \cdot \frac{1}{\left[1-(1+k)^3(1-e)\right]^3}$$

and, $\frac{(1-e)}{d.e^3}$ becomes $\frac{(1+k)^2(1-e)}{d\left[1-(1+k)^3(1-e)\right]^3}$

$$\Delta P = \frac{150.h.VL}{f_s^2}\left[\frac{(1+k)^2(1-e)}{d}\right]^2 \frac{1}{\left[1-(1+k)^3(1-e)\right]^3} + \frac{1.75p.V^2L}{f_s} \frac{(1+k)^2(1-e)}{d\left[1-(1+k)^3(1-e)\right]^3}$$

$$\frac{\Delta P_1}{\Delta P_o} = \frac{150h.V.L}{f_s^2}\left[\frac{(1+k)^2(1-e)^2}{d}\right] \frac{1}{\left[1-(1+k)^3(1-e)\right]^3} + \frac{1.75.p.V^2.L(1+k)^2(1-e)}{f_s.d\left[1-(1+k)^3(1-e)\right]^3}$$

$$\frac{150h.V.L}{f_s^2.d^2} \frac{(1-e)^2}{e^3} + \frac{1.75p.V^2.L(1-e)}{f_s.d.e^3}$$

V is the superficial velocity
p is the fluid density
d is the particles equivalent spherical diameter
k is the fractional diametral increase in particle size
ΔP_0 is the uncorroded pressure drop
ΔP is the corroded pressure drop
h is the fluid viscosity
L is the bed thickness

Example parameters (Table 12) have been used to calculate the pressure drop across SMP filter media with time for corrosion rates of 0.005 and 0.008 µm/hour. The results, plotted in Figure 21, can be used with a maximum allowable pressure drop to give the filter life.

4.4.4.4.2. Life Assessment Predictions for Sintered Metal Fibre Filter Media.

The assessment of the life of Sintered Metal Fibre filter elements used in reverse jet cleaning applications differs from that of Sintered Metal Powder given that structural integrity of the fibres can be maintained. In contrast to SMP the very high porosity of such media, typically 70-85% results in minimum blinding of the media due to corrosion product. Experience has shown that due to the small fibre diameter typically <40µm, structural failure and resultant loss of filtration integrity will occur in advance of blinding.

The primary characteristic that will determine the life of SMF elements is progressive blinding of the filter medium due to particulate ingress into the filter medium. The life of the filter element will be dependent on many factors at both the filter element and systems level; the key factors are defined in Table 13.

As can be clearly seen from the above factors, it is not feasible to define an absolute life of a filter element, as this will be dependant on the specific process operating conditions and design. In addition life predictions are invariably further complicated by changes in the process conditions or failure/ performance of upstream equipment for example heat exchangers etc. that can dramatically affect the blinding rate and life of the filter. This is particularly significant for particulate clean up in the coal/ biomass gasification systems where the technology remains largely in the development/ proving stage and process changes can be frequent.

Based on both plant operating experience and laboratory testing, estimates can be made for the life of a metal fibre element with a defined terminal pressure loss. Data collated from gasification and catalyst recovery applications indicate that typically the process can facilitate a maximum pressure loss across the particulate clean up filter in the region of 40 - 60 KPa.

Life predictions can therefore be made based on the analysis of the "stabilised" region of the pressure loss characteristics and the estimated time to reach the terminal pressure loss. It is worth noting that while theoretically the reverse jet cleaning systems reaches a stabilised pressure loss characteristics experience to-date has shown this to rarely be true and there remains a gradual increase in the pressure loss with time.

Using the Least Square method to determine best fit, predictions have been made of estimated filter life based on laboratory and process plant operating data, this indicates a typical life as follows:

$$\Delta pt = 0.009 \times T + 2758$$

Where Δpt = Terminal pressure loss Pa, and T = Predicted life in hours

Therefore, $$T = \left(\Delta pt - 2758 \right) \div 5.1$$

For a Terminal pressure loss of 50 KPa, the predicted life of a Metal Fibre Element would be:

$T = (50000 - 2758) \div 5.1$ = 9263 hours.

5. SUMMARY

This project has successfully investigated the performance of a range of candidate materials for the manufacture of filters for use in gasifier (IGCC and ABGC) hot gas paths.

The results from Activity A (screening test using high H_2S gas at 450ºC) were used to aid the selection of candidate materials for Activity B. The materials recommended for inclusion in the remaining tests were Haynes D205 EN2691, Fecralloy, HR160, IN690, HA188, Iron Aluminide, IN C276, Hastelloy X and AISI316L (IN800HT and AISI310 will be reference materials).

The Activity B tests have been completed, the specimens examined, oxide thickness measurements made and alloy performance ranked for each of the test conditions. In general the ranking of materials tested in high H_2S (IGCC) gas correspond with those given in Activity A and the damage was greatest on the deposit coated specimens. The damage to alloys exposed in the low H_2S (ABGC) gas test was significantly lower than in the equivalent high H_2S (IGCC) gas test.

Using the results of Activity B, the existing corrosion life prediction models developed at Cranfield University have been modified. It has been demonstrated how to predict the expected service lives and upper temperature limits of filter media under operational IGCC filter conditions.

The design requirements for a prototype element for IGCC/ABGC applications have been identified and related to the data produced in this project. Life prediction models are illustrated for sintered metal fibre and sintered metal powder filter media.

6. RECOMMENDATIONS

Metallic filter elements continue to demonstrate excellent results in numerous coal gasification demonstration/development facilities, however on stream life remains a barrier to the economic exploitation of this technology. Further development of suitable materials remains high on the priority list. The project has provided the basis for new opportunities for the development of metallic filter media in gasification environments. To confirm this potential the manufacture of full sized elements is required together with their demonstration in pilot scale trials and in commercial installations. This will be the subject of a subsequent targeted proposal(s).

In addition to coal, biomass gasification can benefit from the improved reliability and filtration performance offered by metallic filters and it is recommended that further work is undertaken to evaluate materials suitable for operating in such environments.

7. AKNOWLEDGEMENTS

Funding has been provided by UK Department of Trade and Industry (Cleaner Coal Project 201).

8. REFERENCES

1. Takematsu, T. And Maude, C.W., "Coal Gasification for IGCC Power Generation", IEACR/37, IEA Coal Research, London, UK (1991)
2. Proc. Corrosion in Advanced Power Plants, Special Issue of Materials at High Temperatures, 14 (1997)
3. Proc. First International Workshop on Materials for Coal Gasification Power Plant, Petten, The Netherlands, June, 1993, in Materials for Coal Gasification Power Plant, Special Issue of Materials at High Temperature, 11 (1993)
4. Schlachter, W. And Gessinger, G.H., *in* High Temperature Materials for Power Engineering 1990, E Bachelet et al Eds, (Kluwer, 1990) pp. 1-24
5. Oakey, J.E. And Simms, N.J., *in* Materials for Advanced Power Plant 1998, J Lecomte-Beckers et al Eds, (Forschungszentrum Julich GmbH, Germany, 1998) pp. 651-662
6. J van Liere and W T Bakker, in Materials for Coal Gasification Power Plant, Special Issue of Materials at High Temperature, 11, 4-9 (1993).
7. I Mendez-Vigo, J Chamberlain and J Pisa, in Corrosion in Advanced Power Plants, Special Issue of Materials at High Temperatures, 14, 15-20 (1997).
8. Erosion/Corrosion of Advanced Materials for Coal-Fired Combined Cycle Power Generation, Final and Summary Reports on JOUF-0022 (1994).
9. F Gesmundo, in High Temperature Materials for Power Engineering 1990, eds E Bachelet et al, pp67-90, Kluwer, (1990).
10. F Gesmundo, Advanced Materials for Power Engineering Components: The Corrosion of Metallic Materials in Coal Gasification Atmospheres - Analysis of Data from COST 501 (Round 1) Gasification Subgroup. EUCO/MCS/08/1991 (1991).
11. R C John, in Proc. Symposium on Life Prediction of Corrodible Structures, Cambridge, UK, 1991, pp33/1-21, National Association of Corrosion Engineers, Houston, USA (1991).
12. R C John, W C Fort and R A Tait, in Materials for Coal Gasification Power Plant, Special Issue of Materials at High Temperature, 11, 124-132 (1993).
13. SAE J726 – 'Air Cleaner Test Code', Society of Automotive Engineers (SAE), Warrendale, June 1987.
14. ISO 12103-1:1997 – 'Road Vehicles – Test Dust for Filter Evaluation, Part 1: Arizona Test Dust', International Organization for Standardization.

Table 1. Nominal Compositions of Alloys used in Activity A.

Alloy	Composition (wt %)														
	Ni	Cr	Fe	Si	Mo	Cu	W	Mn	Co	Al	Cb+Ta	Ti	B	C	Others
Haynes D205	Bal	20	6	5	2.5	2								0.03*	
Fecralloy		15.0-22.0	Bal	0.2-0.4						4.0-5.2				0.02*	0.05-0.4Y
Haynes HR160	37†	28	3.5*	2.75	1*		1*	0.5	30		1*Cb	0.5		0.05	
Inconel 690	58†	27-31	7-11	0.5*		0.5*		0.5*						0.05*	0.015*S
Inconel 686	Bal	19.0-23.0	1.0*	0.08*	15.0-17.0		3.0-4.4	0.75*				0.02-0.25		0.01*	0.04*P, 0.02*S
Haynes 188	20.0-24.0	21.0-23.0	3.0*	0.20-0.50			13.0-15.0	1.25*					0.015*	0.05-0.15	0.02-0.12La
AISI 310	19-22	24-26	48	1.5				2						0.25	0.045P, 0.03S
Incoloy 803	32.0-37.0	25.0-29.0	Bal	1.0*		0.75*		1.5*				0.15-0.60		0.06-0.10	0.015*S
Haynes G30	43	28.0-31.5	13.0-17.0	0.8*	4.0-6.0	1.0-2.4	1.5-4.0	1.5*	5.0*		0.3-1.5			0.03*	0.04*P, 0.02*S
Haynes 556	20	22	31†	0.4	3		2.5	1	18	0.2	0.6Ta			0.10	0.02La, 0.02Zr,0.20N
Inconel 601	58.0-63.0	21.0-25.0	Bal	0.5*		1.0*		1.0*		1.0-1.7				0.10*	0.015*S
AISI 316L	10-14	16-18	62	1	2-3			2						0.03	0.045P, 0.03S
Incoloy 800HT	30.0-35.0	19.0-23.0	39.5†							0.25-0.60		0.25-0.60		0.06-0.10	
Incoloy C276	57	14.5-16.5	4.0-7.0	0.08*	15.0-17.0		3.0-4.5	1.0*	2.5*					0.01*	0.35*V, 0.025P, 0.010*S
Hastelloy X	47†	22	18	1*	9		0.6	1*	1.5				0.008*	0.10	
Inconel 625	62†	21	5*	0.5*	9			0.5*	1*	0.4*	3.7	0.4*		0.10*	
Haynes 214	75†	16	3					0.5*		4.5			0.01*		0.1*Zr, 0.01Y
Haynes HR120	37	25	33†	0.6	2.5*		2.5*	0.7	3*	0.1	0.7Cb		0.004	0.05	0.020N

Table 2. Test Parameters for Activity A and B
***High = IGCC and Low = ABGC**

Activity	Test	Time (hrs)	Temp (°C)	Gas H_2S Level*	Deposit	Re-coat (hrs)
A	Screening	1000	450	High	No	-
B	1	3000	450	High	Yes	1000
	2	1000	550	High		
	3		550	Low		
	4		500	High		

Table 3. Gas Composition used in Tasks 1 and 2

Gas	Gas Compositions (vol.%)							
	CO	**CO_2**	**H_2**	**H_2S**	**H_2O**	**HCl**	**CH_4**	**N_2**
'High H_2S'	61.0	4.00	31.0	1.00	3.00	0.04	-	-
'Low H_2S'	18.0	8.40	14.7	0.02	10.40	0.06	2.5	45.92

Table 4. Weight Gain Results for Activity A Screening Test.
(Note the calculation of surface area does not include an allowance for cap and root of welds)

Alloy	**(mg/cm^2)**	**Weld**	**Weight change reliable?**
Haynes D205 EN2691	0.040	No	Yes
Fecralloy oxidised	0.072	No	Yes
Fecralloy	0.118	No	Yes
Haynes HR160	0.327	Yes	Yes
Incoloy alloy 803 pickled	3.459	No	Yes but ~ 5% corrosion layers detached
Haynes 188	3.631	Yes	Yes
Inconel 690 pickled	3.822	No	Yes
Inconel 686	5.634	No	Yes
AISI 310	7.607	No	Yes
Haynes G30	7.742	Yes	Yes
Inconel 625 pickled	9.359	No	Yes
Incoloy C276 pickled	14.026	No	Yes
Haynes 214	20.202	Yes	Borderline ~ 40% corrosion layers detached
Haynes HR120	-32.361	Yes	No
Hastelloy X	-13.541	Yes	No
Incoloy 800HT pickled	-5.084	No	No
Haynes 556	2.839	Yes	No
Inconel 601 pickled	3.794	Yes	No
AISI 316L	8.761	No	No

Table 5. Measured Oxide and Sulphide Thickness from Samples Exposed in Screening Test (Activity A).

Alloy	Parent or Weld	Oxide Thickness (mm)		Sulphide Thickness (mm)		Comments
		Typical	Max	Typical	Max	
Haynes D205	Parent	see	comment	-	-	2µm oxide and/or sulphide. Small number of discrete areas of minimal corrosion.
Fecralloy oxidised	Parent	-	2	-	2	Small number of discrete areas of minimal corrosion.
Fecralloy	Parent	see	comment	-	-	2µm oxide and/or sulphide. Small number of discrete areas of minimal corrosion.
Haynes HR160	Parent	2	5	4	20	Discrete regions of corrosion.
	Weld	see	comment	-	-	Similar to parent but with internal oxide (two oxide types occurring together).
Inconel 690	Parent	10	22	14	24	
Inconel 686	Parent	10	34	14	32	
Haynes 188	Parent	12	17	40	-	Uniform oxide. Sulphide very fragmented on outer edge.
	Weld	see	comment	-	-	Little oxide/sulphide visible but surface appears pitted.
AISI 310	Parent	12	62	38	62	Oxide and sulphide attached but sulphide fragmented on outer edge.
Incoloy alloy 803	Parent	20	24	34	86	Sulphide very fragmented.
Haynes G30	Parent	20	34	38	-	Metal/oxide interface irregular. Sulphide mainly detached from oxide.
	Weld	see	comment	-	-	Little oxide/sulphide but it appears that there was less corrosion than parent
Haynes 556	Parent	24	-	38	-	Uniform oxide, sulphide detached and split into two layers (outer mainly lost)
	Weld	20	-	-	-	Similar to parent except sulphide lost.
Inconel 601	Parent	24	30	32	52	
	Weld	24	30	32	52	
AISI 316L	Parent	26	38	58	76	Sulphide/oxide uniform and attached.
Incoloy 800HT	Parent	32	34	40	-	Very uniform oxide layer. Sulphide mainly attached but outer edge fragmented.
Incoloy C276	Parent	32	88	38	120	Sulphide detached from oxide and fragmented at outer edge.
Hastelloy X	Parent	34	38	-	-	Two oxide layers containing sulphides, main sulphide layer lost.
	Weld	58	72	-	-	
Inconel 625	Parent	34	42	28	108	Oxide very uniform. Sulphide detached from oxide.
Haynes 214	Parent	100	126	-	-	Sulphide very fragmented, not measured.
	Weld	78	88	-	-	Sulphide very fragmented, not measured.
Haynes HR120	Parent	see	comment	-	-	Oxide/sulphide lost from specimen.
	Weld	40	58	70	-	Sulphide attached to oxide, but fragmented at outer edge.

Table 6. Materials for Activity B
SMP = Sintered Metal Powder, OD = Outer Diameter

No	Material	Type	Deposit	Type	Size (mm)
1	AISI 316L	SMP	Y	Ring	~20 OD37
2	Hastelloy X	SMP	Y	Ring	~20 OD37
3	Haynes HR160	-	Y	Coiled wire	~1 (dia)
4	Haynes 188	-	Y	Coiled wire	~1 (dia)
5	Haynes D205 EN2691	-	Y	Coiled wire	~1 (dia)
6	Hastelloy C276	-	Y	Mesh	-
7			N		
8	Fecralloy	-	Y	Fibre media	-
9			N		
10	Iron Aluminide	-	Y	Solid disc	~52 (dia)
11	Alloy 800HT	-	Y	Plate	-
12	AISI 310	-	Y	Plate	-
13	IN 690	-	Y	Disc (rod)	-

Table 7. Deposit Compositions for Activity B

Deposit	Deposit Compositions (wt.%)						
	Flyash	Char	NaCl	KCl	$FeCl_2$	PbS	ZnS
'High H_2S'	90	-	2	1	2	4	1
'Low H_2S'	-	90	2	1	2	4	1

Table 8. Typical & Maximum Measured Oxide Thickness for Activity B Test Specimens with Applied Deposit († only 2000 hours, * equivalent to 100% oxidation)

Material	Typical (Typ) & Maximum (Max) Measured Oxide Thickness (µm)							
	Test 1		Test 2		Test 3		Test 4	
	Typ	Max	Typ	Max	Typ	Max	Typ	Max
AISI 316L	50	60	15	40	10	25	10	45
Hastelloy X†	80*	80*	25	70	<1	2	80*	80*
Haynes HR160	1	4	6	12	<1	1	3	6
Haynes 188	18	20	20	37	2	6	14	20
Haynes D205	<1	2	12	20	<1	3	1	3
Hastelloy C276	32	38	24	32	<1	4	32	42
Fecralloy	2	7	<1	5	1	6	1	4
Iron Aluminide	6	40*	15*	40*	6	20	8	22
Alloy 800HT	24	35	60	76	2	2	50	64
AISI 310	8	24	12	14	2	14	10	20
IN 690	45	95	35	65	3	6	15	125

Table 9. Typical & Maximum Measured Oxide Thickness for Activity B Specimens without Applied Deposit († only 2000 hours, * equivalent to 100% oxidation, ‡ specimen that replaced Hastelloy X for final 1000 hours in Test 1)

Material	Typical (Typ) & Maximum (Max) Measured Oxide Thickness (µm)							
	Test 1		Test 2		Test 3		Test 4	
	Typ	Max	Typ	Max	Typ	Max	Typ	Max
AISI 316L	43	60	15	35	<1	2	10	25
	8 ‡	35 ‡	n/a	n/a	n/a	n/a	n/a	n/a
Hastelloy X†	80*	80*	60	80*	<1	2	80*	80*
Haynes HR160	<1	3	2	4	<1	<1	6	8
Haynes 188	10	12	30	32	<1	3	14	20
Haynes D205	<1	2	3	8	<1	<1	1	2
Hastelloy C276	22	32	44	48	<1	<1	22	25
Fecralloy	2	6	<1	4	<1	4	<1	4
Iron Aluminide	4	20	15*	40*	4	6	<1	<1
Alloy 800HT	24	35	35	50	<1	<1	30	35
AISI 310	6	15	6	12	2	14	10	18
IN 690	25	36	75	125	3	6	25	45

Table 10. Comparison of Material Performance Rankings for Tasks 1 and 2 Including Mean Rankings for Activity B Tests 1, 2 & 4 with Applied Deposit. (n/a indicates material not tested in Activity A)

Alloy	Activity A	Activity B				Test 1, 2 & 4 Mean
		Test 1	Test 2	Test 3	Test 4	
Hastelloy X	15	11	8	2	9	9.3
IN 690	4	9	10	9	8	9
IN 800HT	13	7	9	6	11	9
IN C276	14	8	7	4	10	8.3
AISI 316L	12	10	5	11	7	7.3
Iron Aluminide	n/a	4	11	10	4	6.3
HA 188	6	6	6	7	6	6
AISI 310	7	5	3	8	5	4.3
HR 160	3	2	2	1	3	2.3
Fecralloy	2	3	1	5	2	2
HA D205 EN2691	1	1	4	3	1	2

Table 11. Comparison of Material Performance Rankings for Tasks 1 and 2 Including Mean Rankings for Activity B Tests 1, 2 & 4 without Applied Deposit. (n/a indicates material not tested in Activity A)

Alloy	Activity A	Activity B				Test 1, 2 & 4 Mean
		Test 1	Test 2	Test 3	Test 4	
Hastelloy X	15	11	10	2	11	10.7
IN 690	4	9	8	6	9	8.7
IN 800HT	13	8	7	1	10	8.3
IN C276	14	7	9	1	8	8
AISI 316L	12	10	5	2	6	7
HA 188	6	6	6	3	7	6.3
Iron Aluminide	n/a	4	11	7	1	5.3
AISI 310	7	5	4	5	5	4.7
HR 160	3	2	2	1	4	2.7
HA D205 EN2691	1	1	3	1	3	2.3
Fecralloy	2	3	1	4	2	2

Table 12. Variables used to Produce Example Life Plot (Figure 21).

Variables	Values	Units
Bed depth	0.02	m
Gas viscosity	3×10^{-05}	Pas
Equivalent particle diameter	0.002	m
Voidage fraction	0.25	-
Gas density	0.5	kg/m^3
Shape factor	1	-
Superficial velocity	0.1	m/s
Uncorroded pressure loss	85.2	Pa

Table 13. Key Factors Controlling the Life of a Filter Element.

Filter Element/ System Level	Process Level
Media Structure	Terminal Pressure Loss
Surface Filtration Effect	Particulate Size Distribution
Permeability	Particulate Adhesive / Cohesive Properties
Reverse Jet Cleaning Frequency	Particulate Concentration
Cleaning Effectiveness	Plant upset conditions

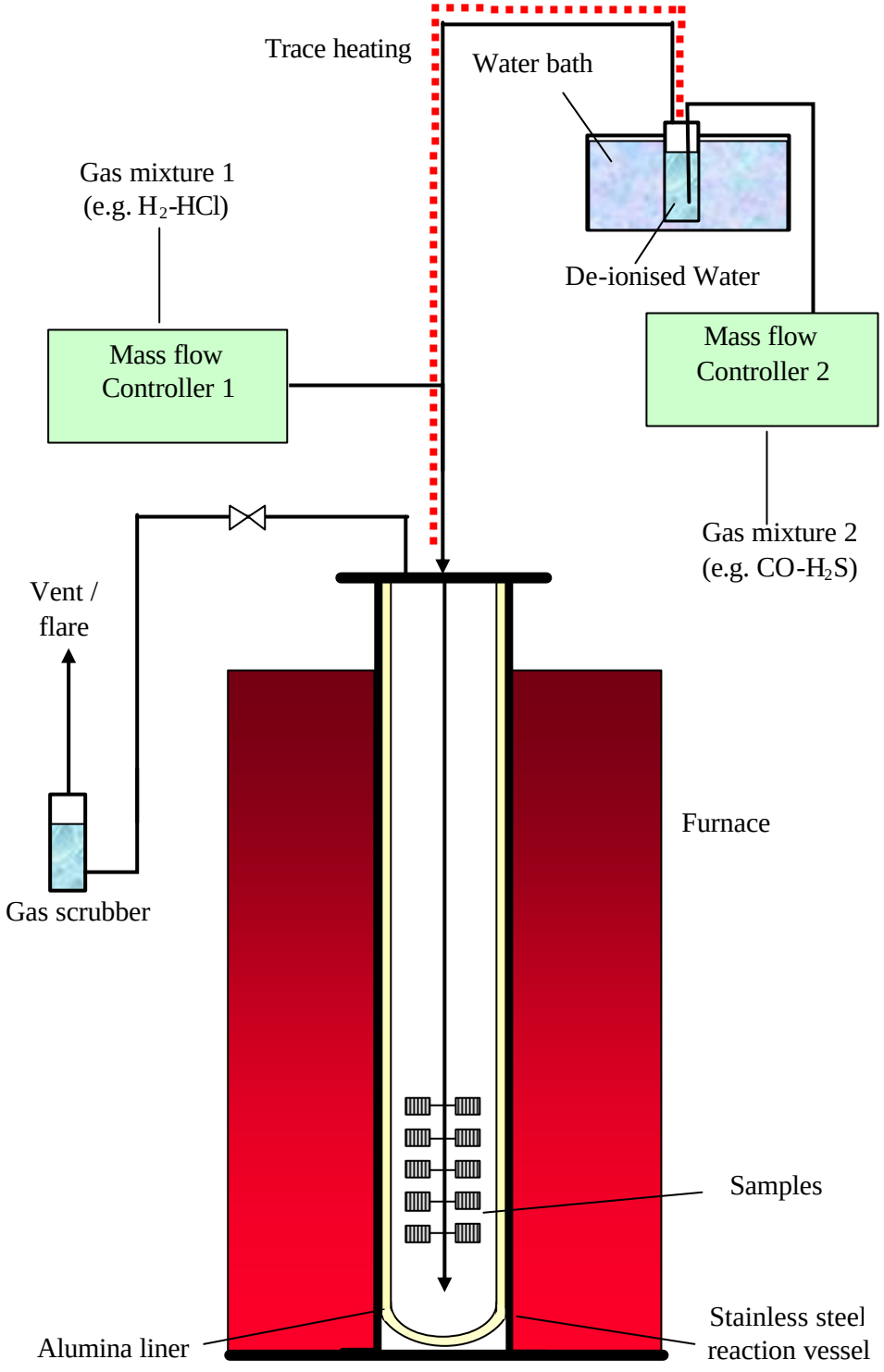

Figure 1. Schematic Diagram of a Controlled Atmosphere Furnace

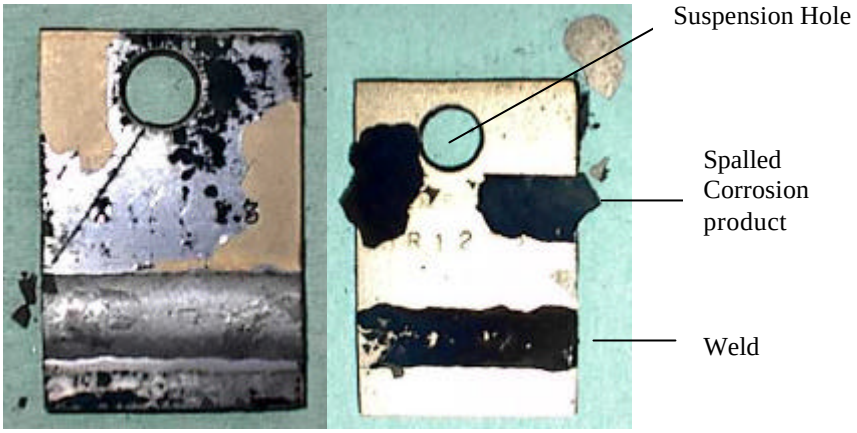

Figure 2. Example of Specimens after initial screening demonstrating where corrosion layers have spalled (Hastelloy X left, HR120 right)

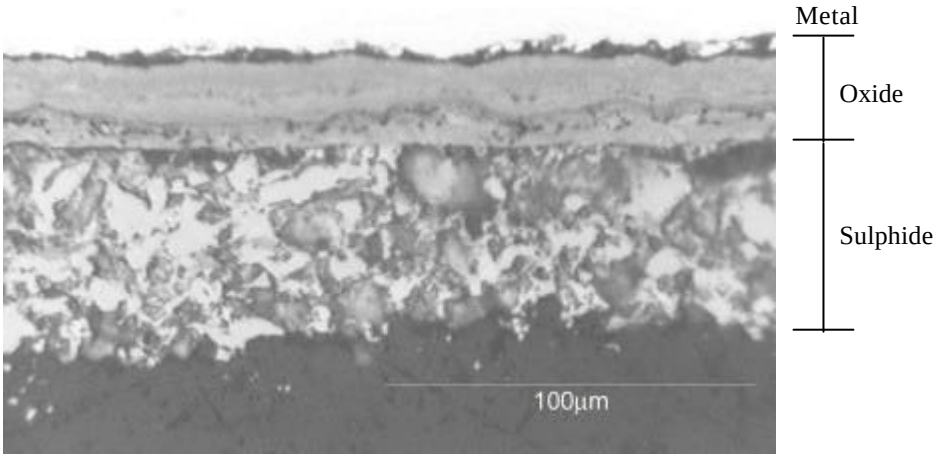

Figure 3. Cross section of 316L specimen after screening test showing oxide and sulphide layers.

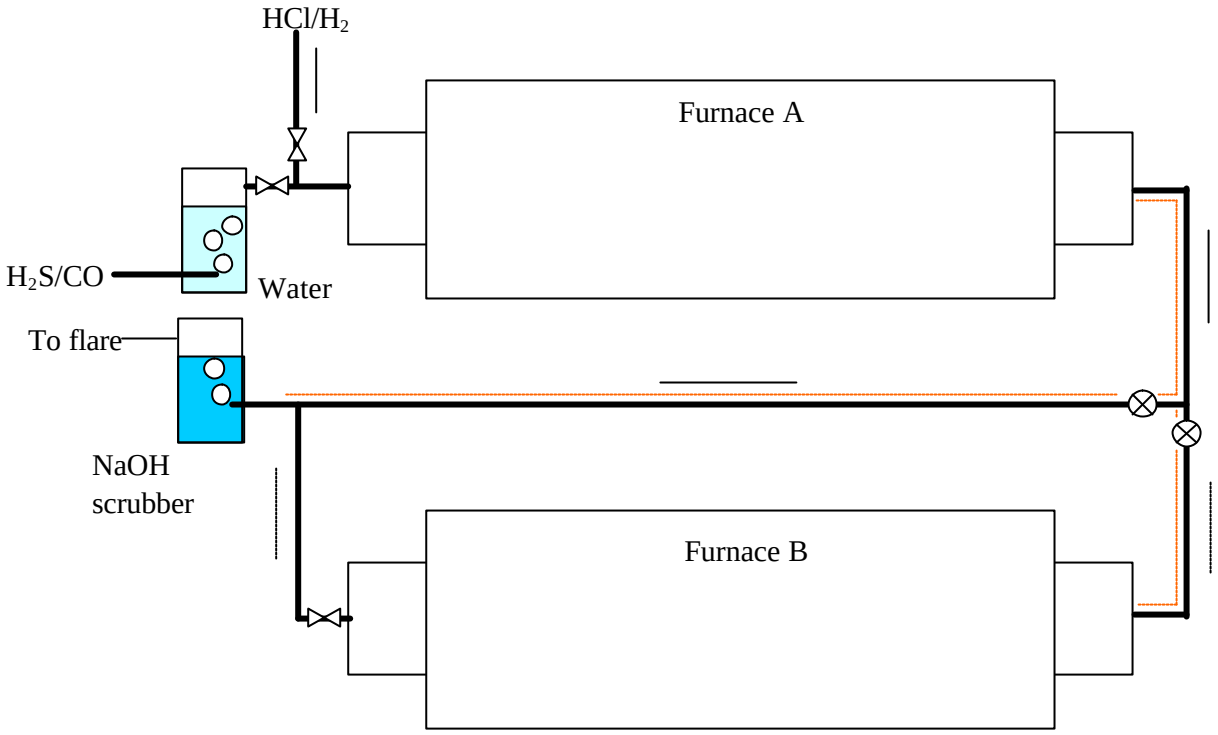

Figure 4. In-Series Horizontal Furnaces (High H_2S)

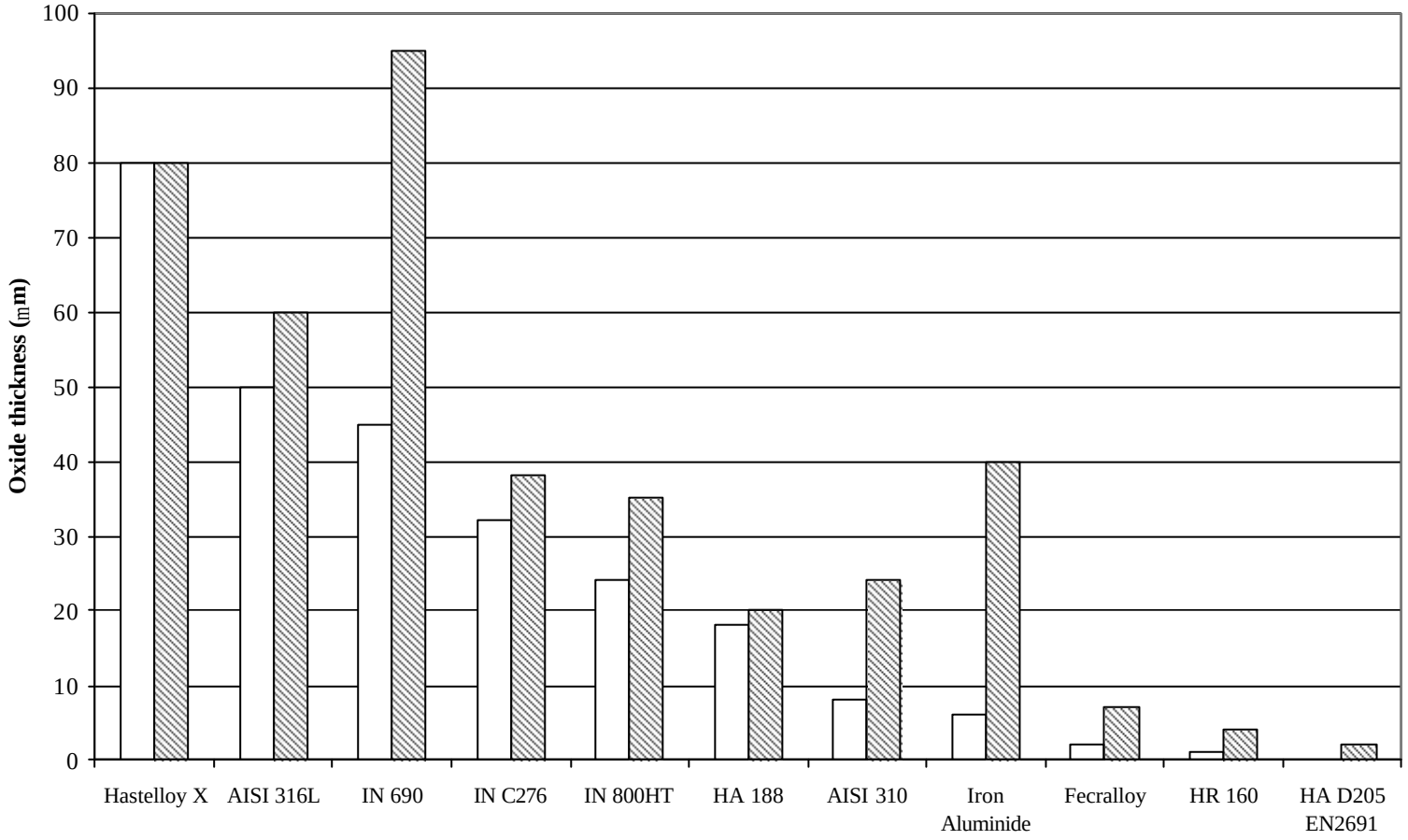

Figure 5. Comparison of Typical (Unshaded) and Maximum (Shaded) Oxide Thickness Measurements for Activity B Test 1 (450ºC, 3000 hours, High H_2S Gas and Applied Deposit (Hastelloy X only 2000 hours)) Left to Right Order of Materials is Lowest to Highest Ranking from Table 10. Where No Bar is Shown this Indicates a Measurement of <1µm.

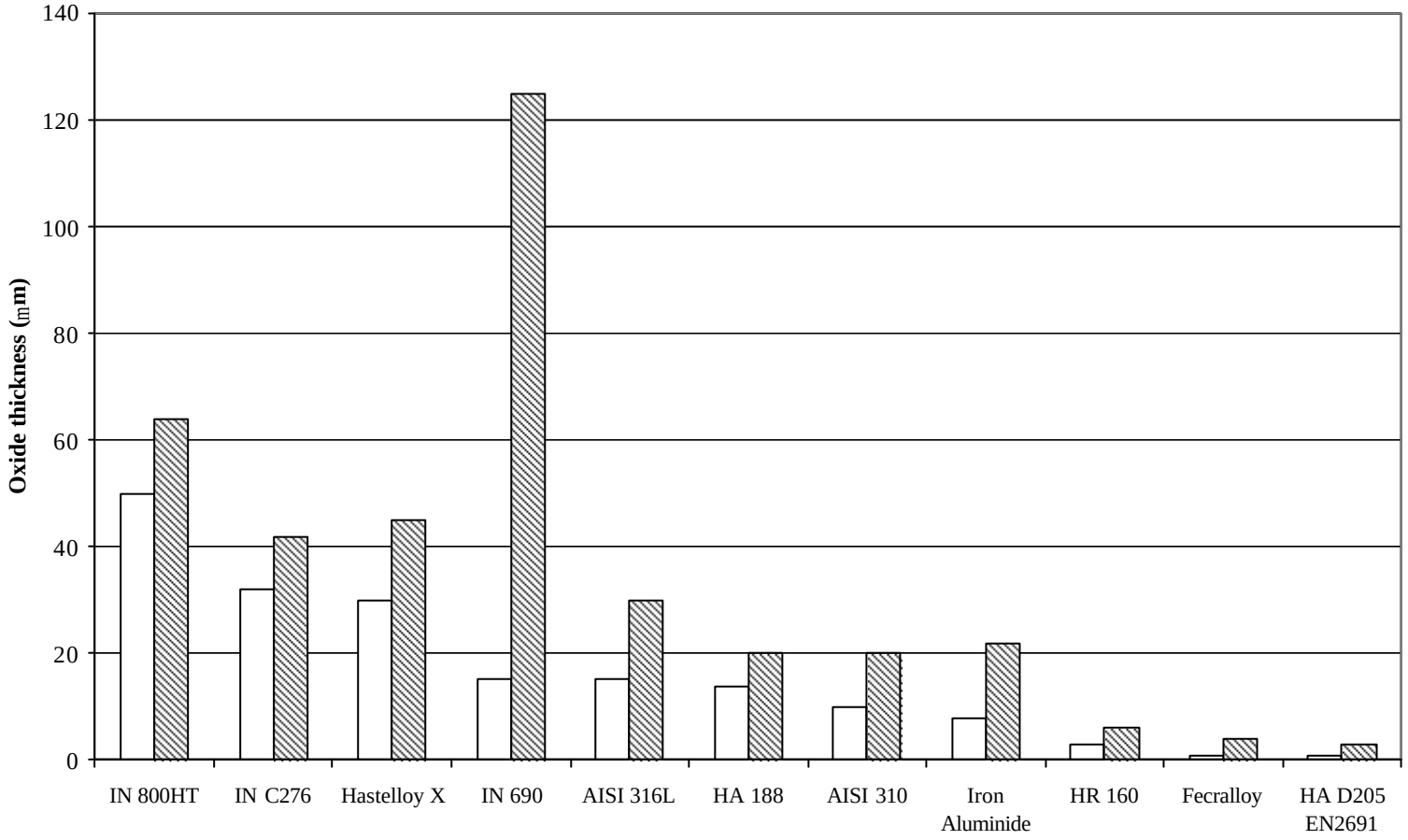

Figure 6. Comparison of Typical (Unshaded) and Maximum (Shaded) Oxide Thickness Measurements for Activity B Test 4 (500°C, 1000 hours, High H_2S Gas and Applied Deposit)
Left to Right Order of Materials is Lowest to Highest Ranking from Table 10.
Where No Bar is Shown this Indicates a Measurement of <1µm.

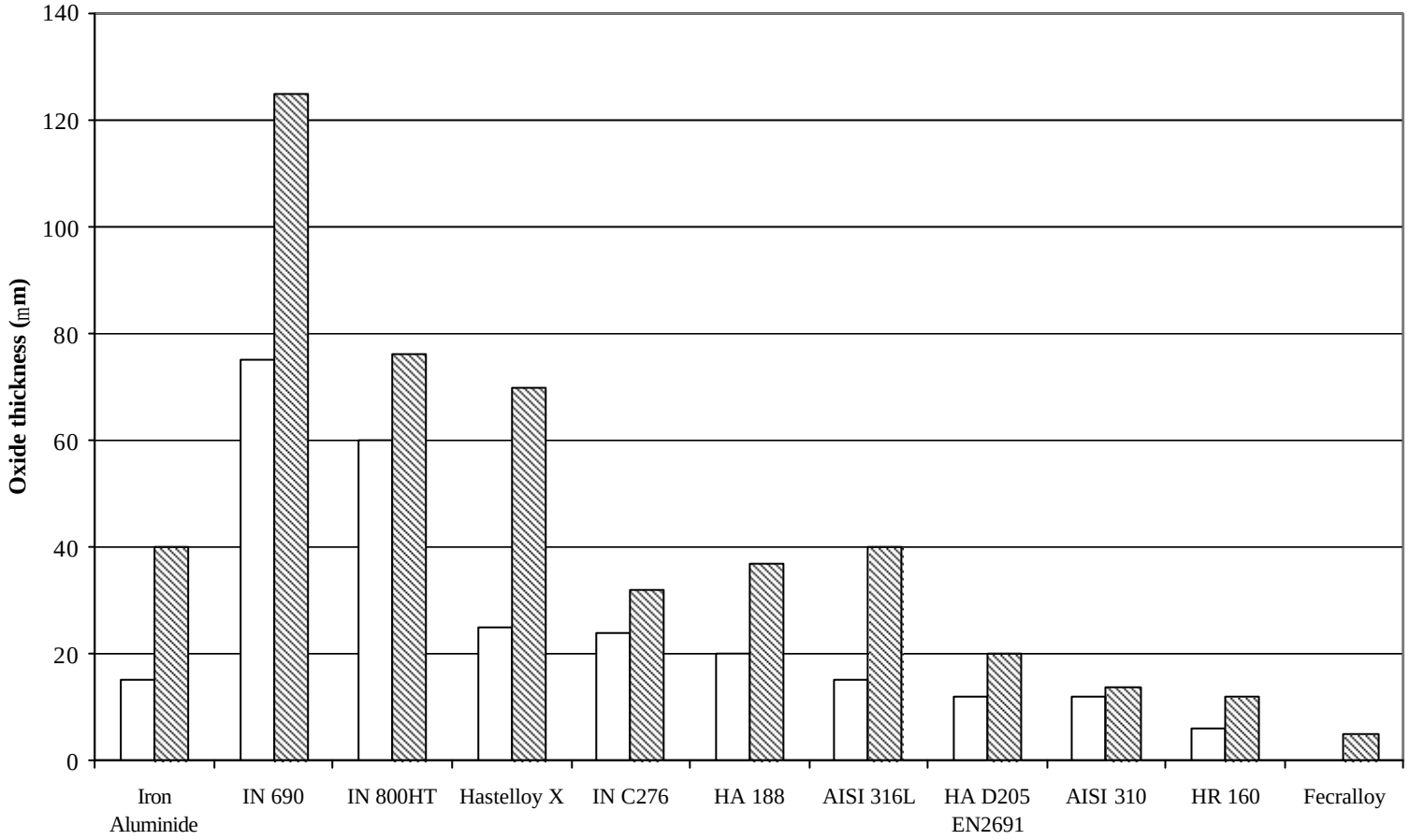

Figure 7. Comparison of Typical (Unshaded) and Maximum (Shaded) Oxide Thickness Measurements for Activity B Test 2 (550°C, 1000 hours, High H_2S Gas and Applie d Deposit)
Left to Right Order of Materials is Lowest to Highest Ranking from Table 10.
Where No Bar is Shown this Indicates a Measurement of <1µm.

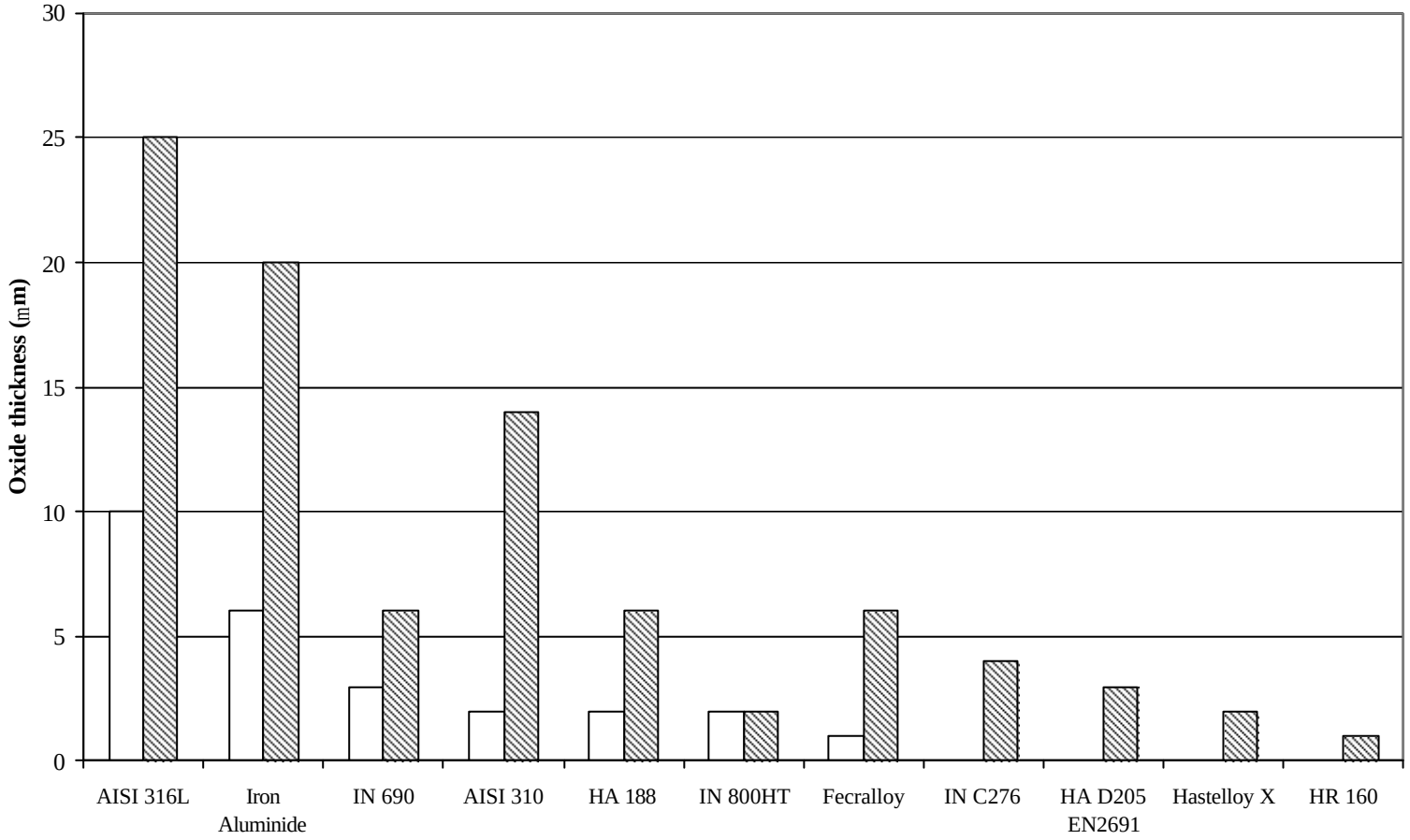

Figure 8. Comparison of Typical (Unshaded) and Maximum (Shaded) Oxide Thickness Measurements for Activity B Test 3 (550°C, 1000 hours, Low H_2S Gas and Applied Deposit)
Left to Right Order of Materials is Lowest to Highest Ranking from Table 10.
Where No Bar is Shown this Indicates a Measurement of <1µm.

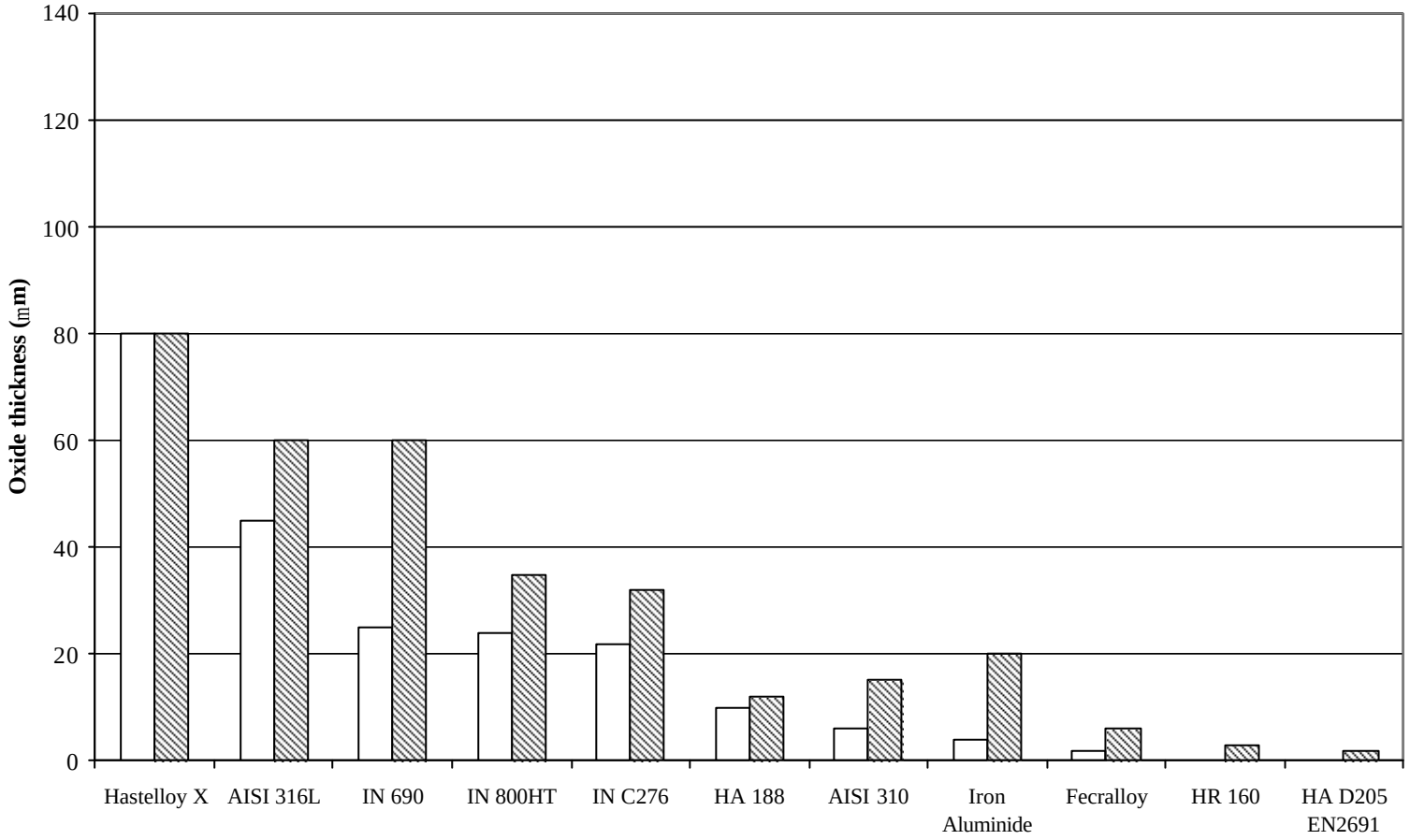

Figure 9. Comparison of Typical (Unshaded) and Maximum (Shaded) Oxide Thickness Measurements for Activity B Test 1 (450ºC, 3000 hours, High H_2S Gas and no Applied Deposit (Hastelloy X only 2000 hours)) Left to Right Order of Materials is Lowest to Highest Ranking from Table 11. Where No Bar is Shown this Indicates a Measurement of <1µm.

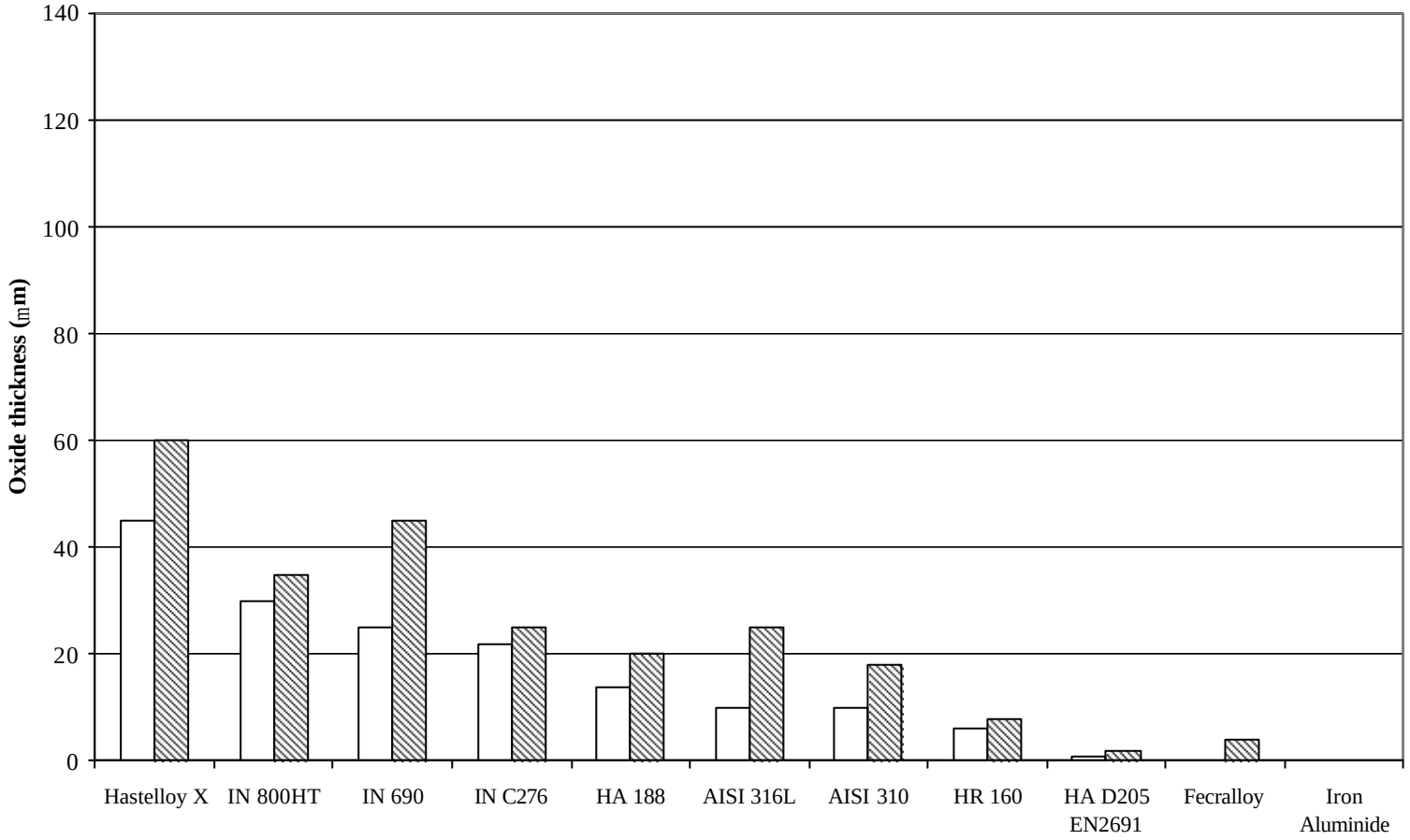

Figure 10. Comparison of Typical (Unshaded) and Maximum (Shaded) Oxide Thickness Measurements for Activity B Test 4 (500ºC, 1000 hours, High H_2S Gas and no Applied Deposit)
Left to Right Order of Materials is Lowest to Highest Ranking from Table 11.
Where No Bar is Shown this Indicates a Measurement of <1µm.

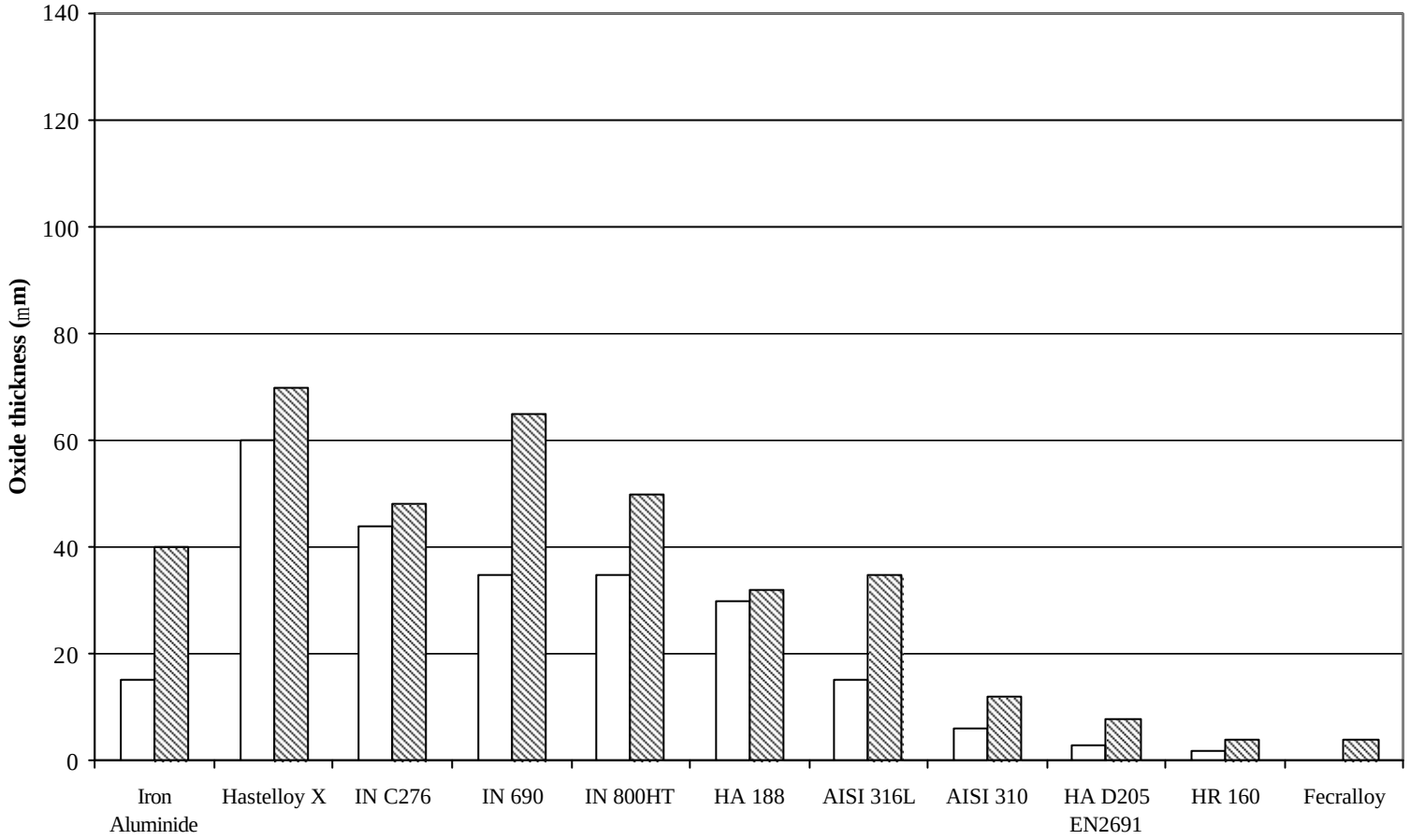

Figure 11. Comparison of Typical (Unshaded) and Maximum (Shaded) Oxide Thickness Measurements for Activity B Test 2 (550ºC, 1000 hours, High H_2S Gas and no Applied Deposit)
Left to Right Order of Materials is Lowest to Highest Ranking from Table 11.
Where No Bar is Shown this Indicates a Measurement of <1µm.

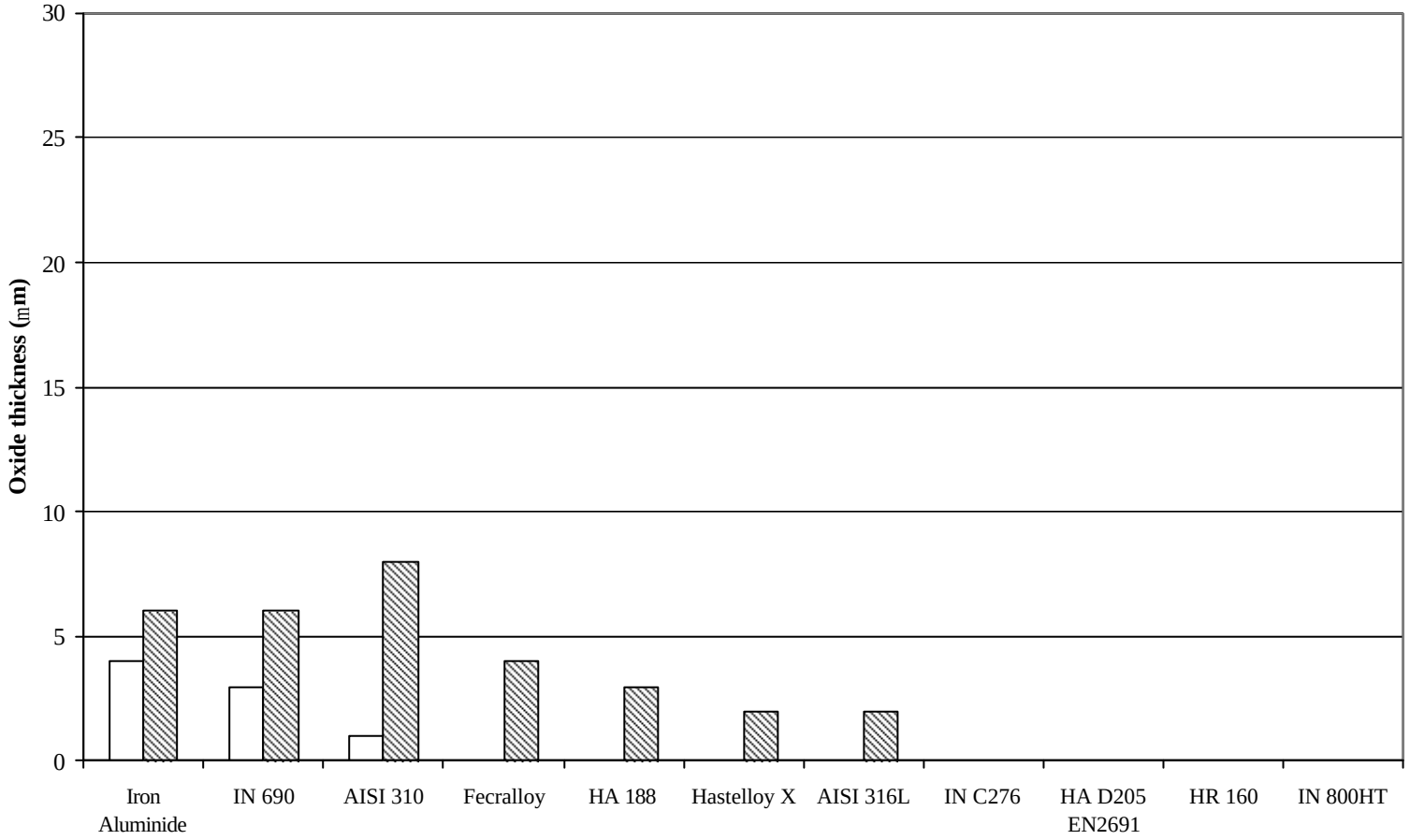

Figure 12. Comparison of Typical (Unshaded) and Maximum (Shaded) Oxide Thickness Measurements for Activity B Test 3 (550°C, 1000 hours, Low H_2S Gas and no Applied Deposit)
Left to Right Order of Materials is Lowest to Highest Ranking from Table 11.
Where No Bar is Shown this Indicates a Measurement of <1μm.

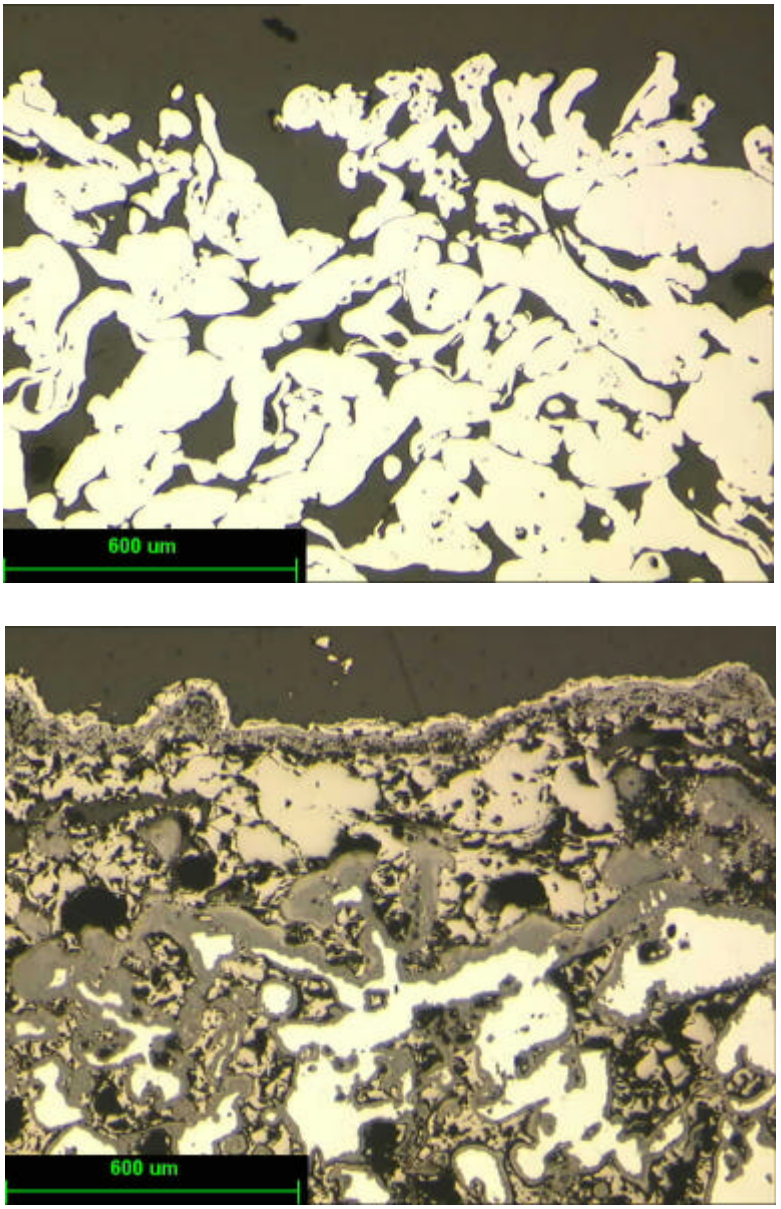

Figure 13. AISI 316L SMP, top reference sample & bottom Activity B, Test 2 sample

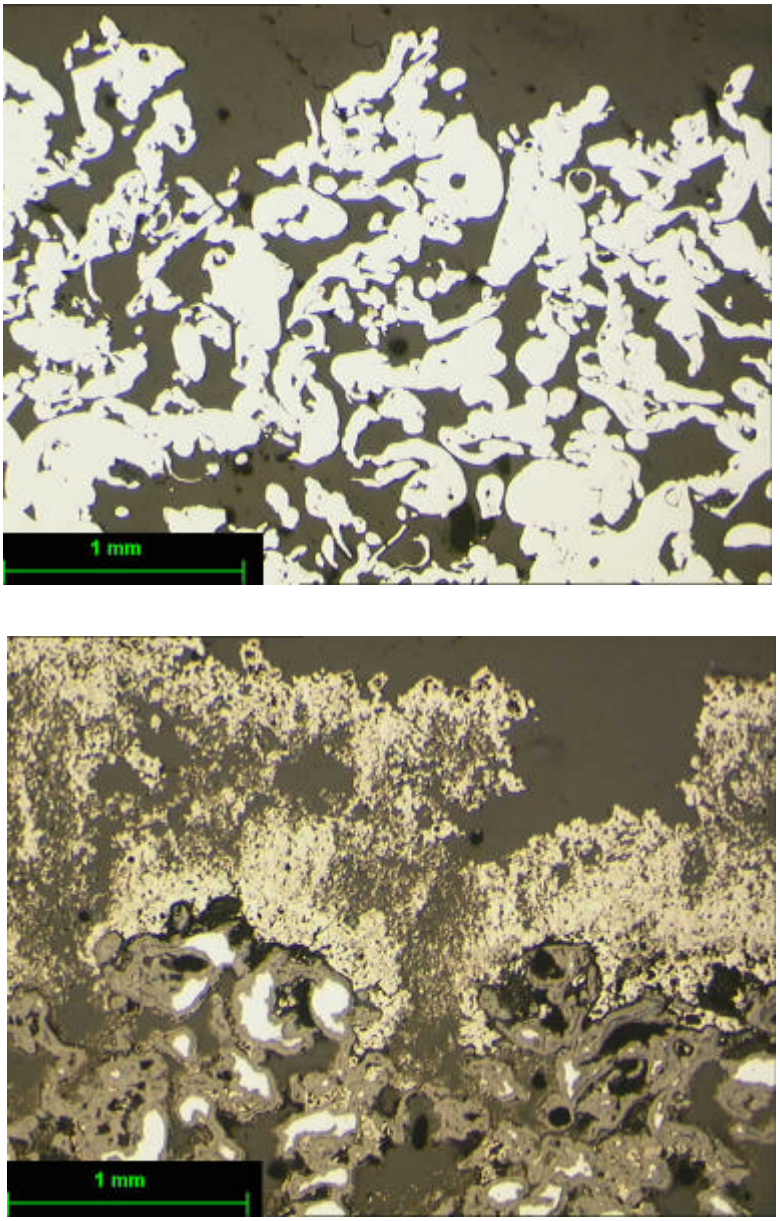

Figure 14. - Hastelloy X SMP, top reference sample , bottom Activity B, Test 2 sample.

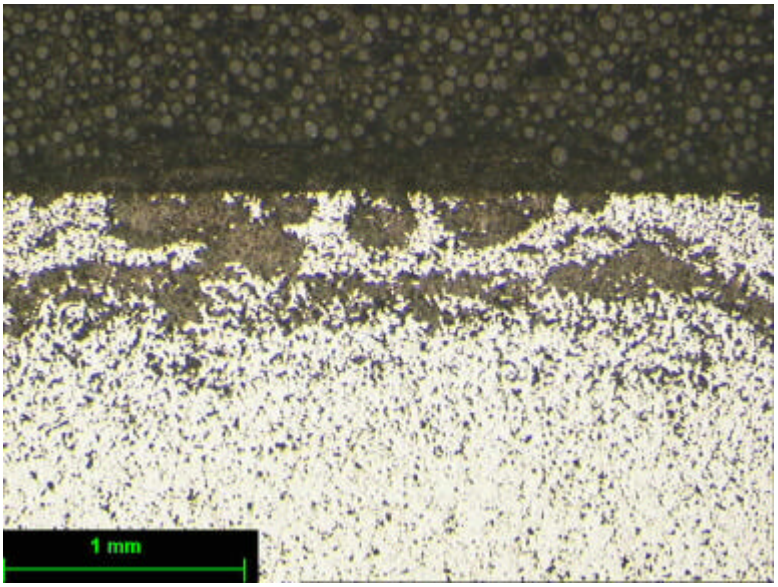

Figure 15. Iron Aluminide, Activity B, Test 2 sample.

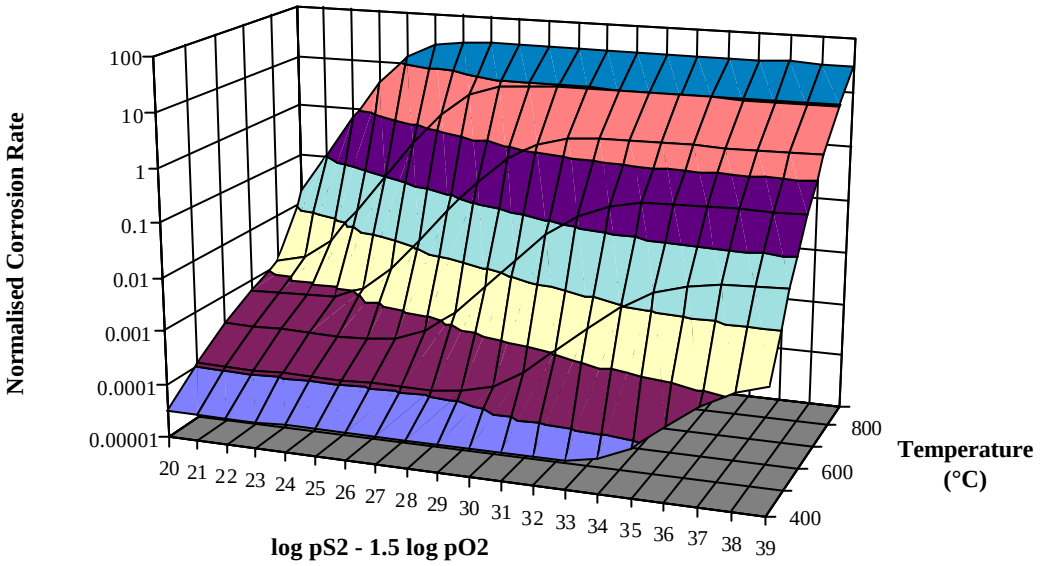

Figure 16. Corrosion Behaviour Modelling of AISI 310 in Gasification Environments

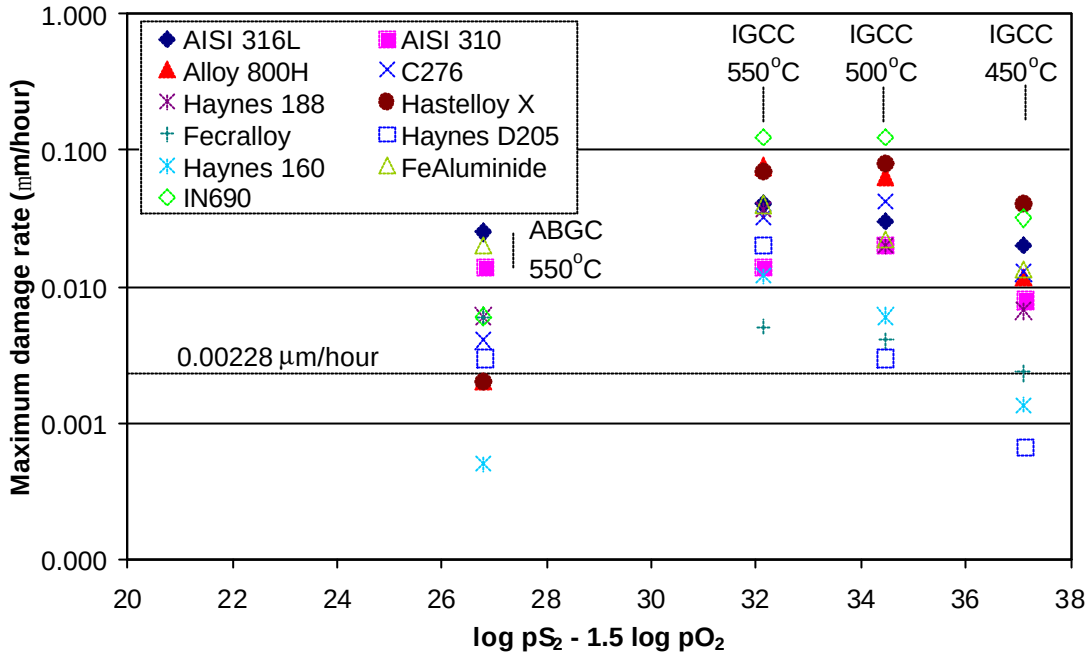

Figure 17. Model Prediction using Activity B Maximum Damage with Deposit Data.

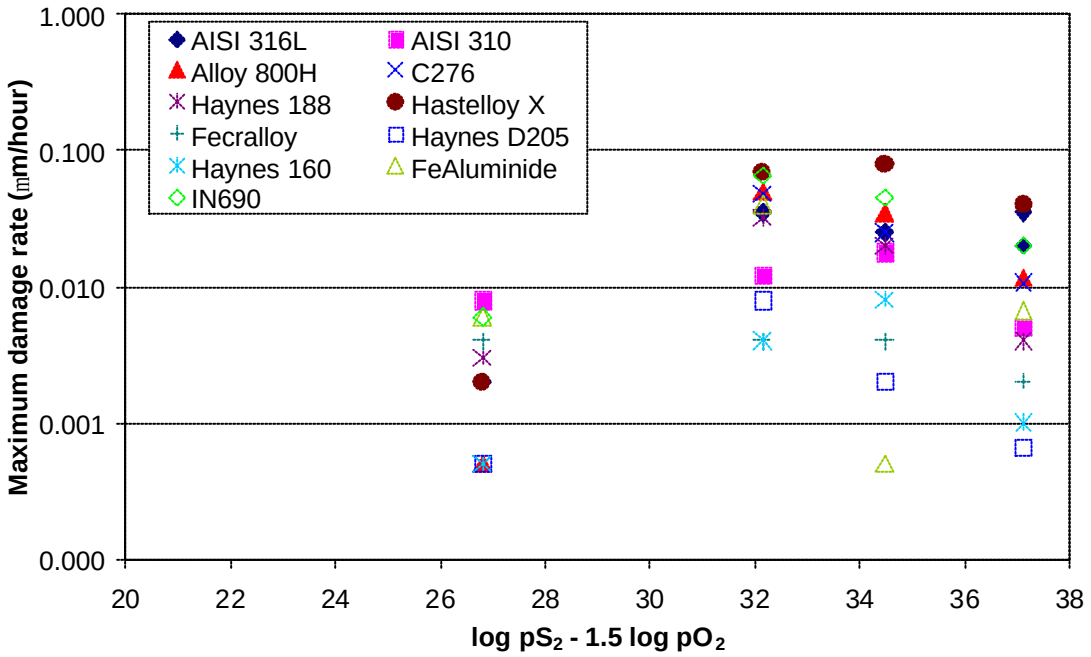

Figure 18. Model Prediction using Activity B Maximum Damage without Deposit Data.

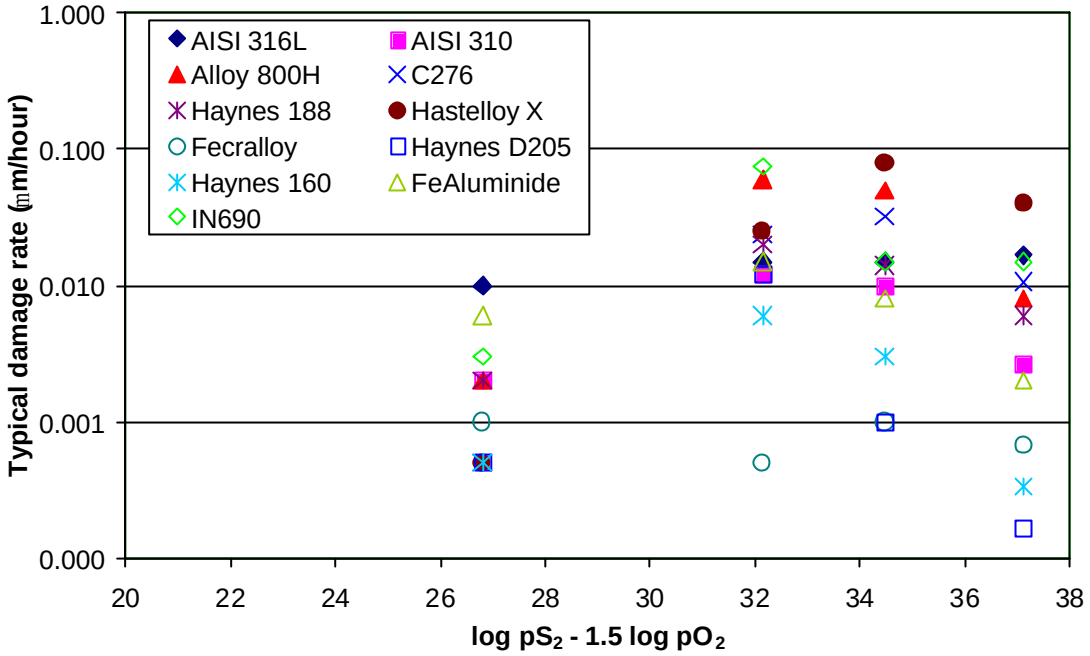

Figure 19. Model Prediction using Activity B Typical Damage with Deposit Data.

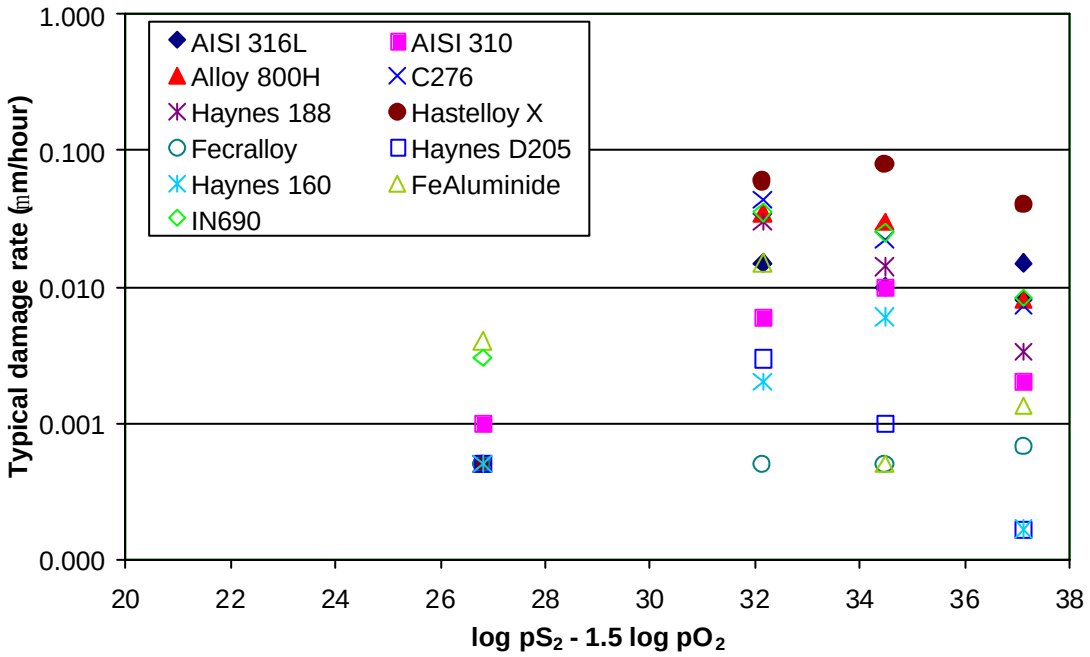

Figure 20. Model Prediction using Activity B Typical Damage without Deposit Data.

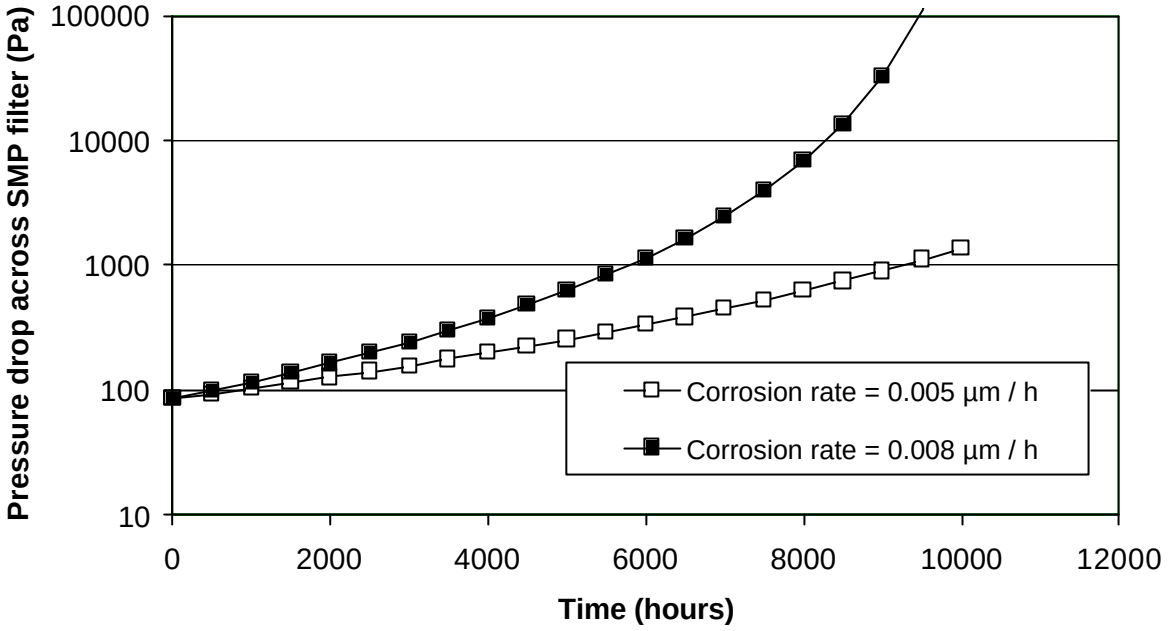

Figure 21. Example of Life Plot for SMP Filter for Two Corrosion Rates.

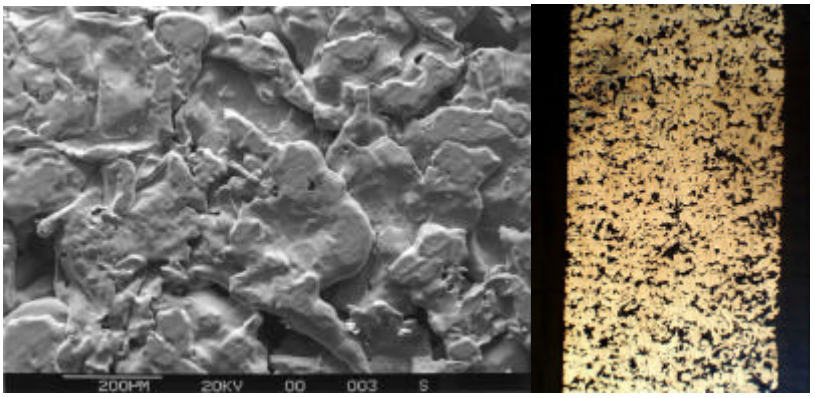

Figure 22. Low Porosity Structure of SMP Media.

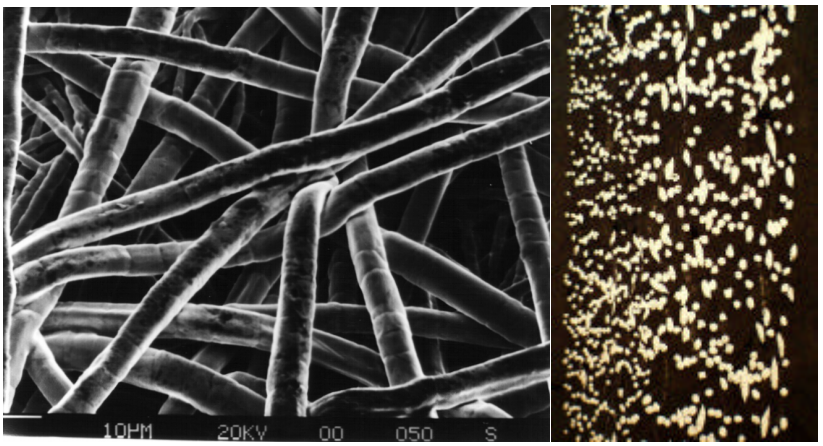

Figure 23. High Porosity of SMF Media.

Figure 24. A set of Hot Gas filter Elements Made Using SMF Media.

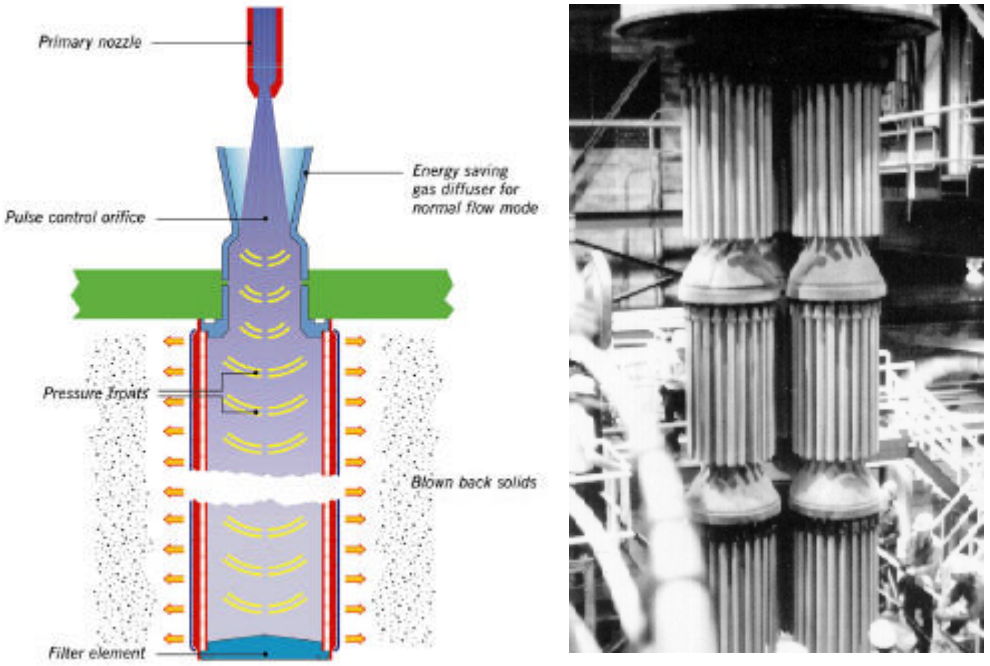

Figure 25. Diagram and Photograph Showing Candles Fitted with a Pulsed Jet Nozzle.

Figure 26. High Speed Photography Showing the Action of Pulsed Jet Cleaning. (Moving across the photograph from left to right: the metal fibre element loaded with dust; the dust is removed from the surface by the pulsed jet action; the dust is carried away; the dust begins to settle; and quickly falls to the bottom of the vessel leaving a clean element. Sequence time - half a second.)

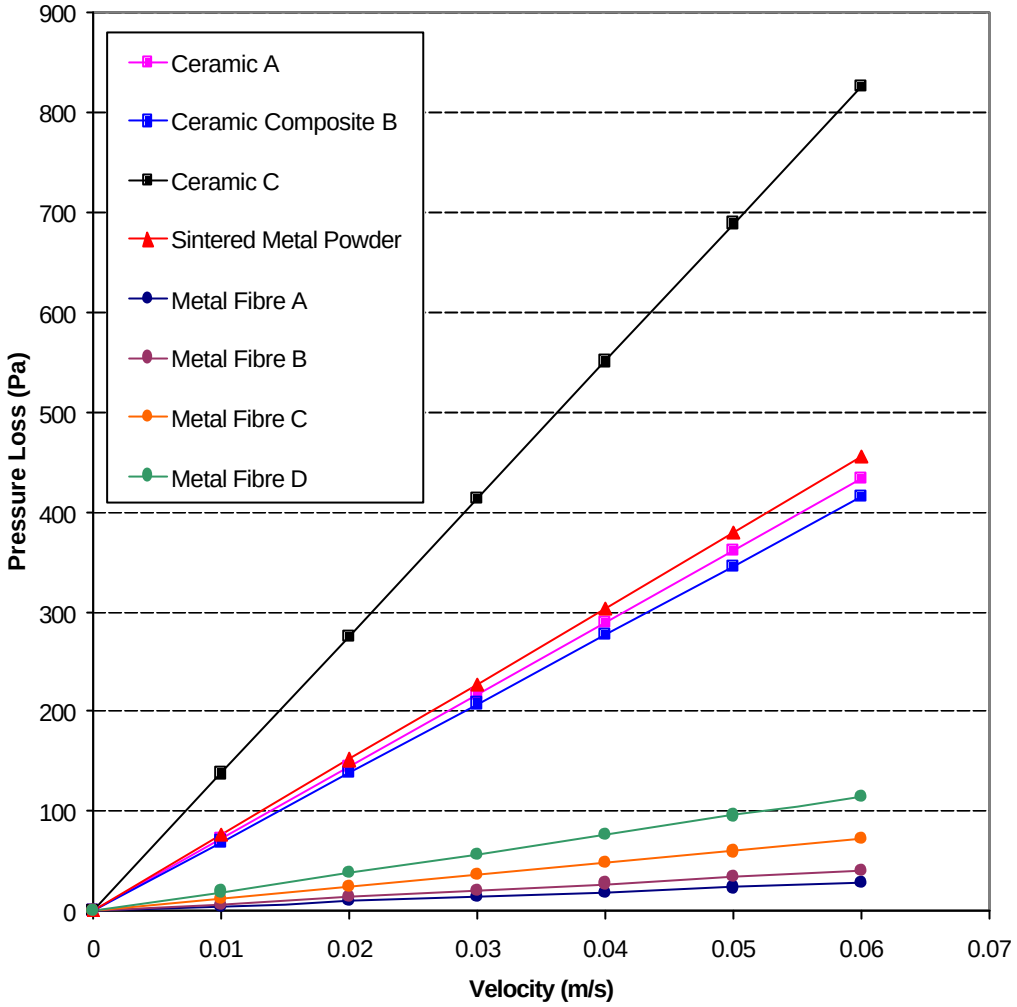

Figure 27. Plot Showing Comparative Pressure Loss Characteristics.

Figure 28. Testing of Filter Elements Using Dust Feeder Connected to Test Rig.

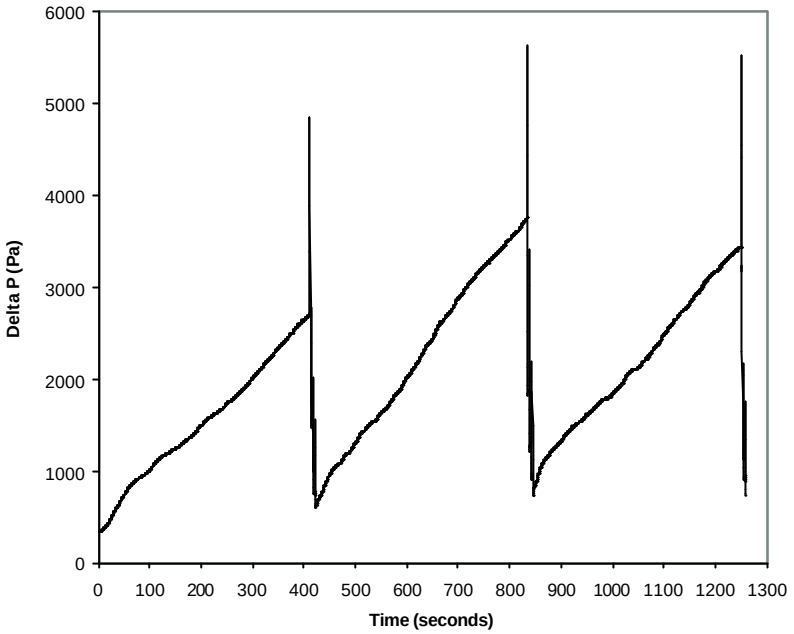

Figure 29. Plot of Differential Pressure Against Time Showing Reverse Pulse Cleaning Cycle.

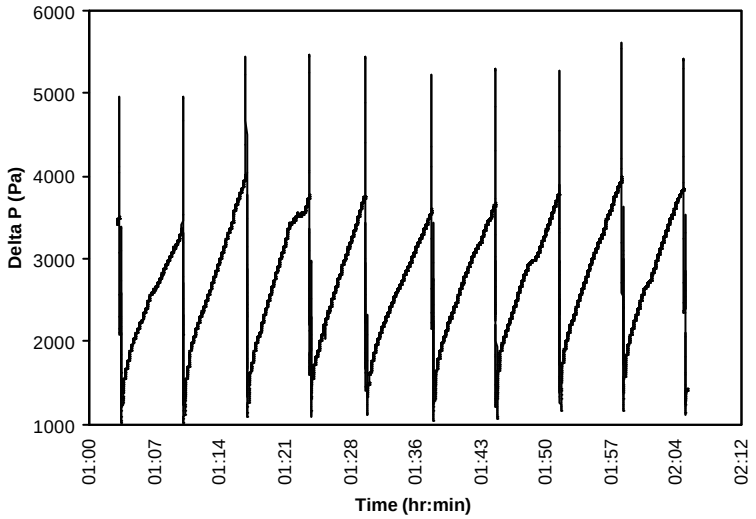

Figure 30. Plot of Differential Pressure Against Time Showing Reverse Jet Cleaning.